Developing Mining Camp Exploration Concepts and Technologies – Brownfield Exploration Project 2013–2016
Edited by Soile Aatos
Geological Survey of Finland, Special Paper 59, 67–96, 2016

# PETROPHYSICAL PARAMETERS AND POTENTIAL FIELD MODELLING IN THE OUTOKUMPU BELT

*by*

*Hanna Leväniemi*

**Leväniemi, H. 2016.** Petrophysical parameters and potential field modelling in the Outokumpu Belt. *Geological Survey of Finland, Special Paper 59*, 67–96, 23 figures and 6 tables.

The Outokumpu and Miihkali regions have been extensively covered by drilling and geophysical ground surveys. The work presented in this paper aimed at defining suitable parameters and methods for modelling the responses of deep-set bedrock features in gravity and magnetic (i.e. potential field) datasets in the Outokumpu region in order to study the depth ranges, dimensions and characteristics of the anomaly sources. The first part of this paper considers the typical petrophysical parameters for the various Outokumpu region rocks from both outcrop and drill core sample data and the second part illustrates the application of these parameters with modelling examples (with emphasis on gravity data).

Results from 2D/3D forward modelling and inversion demonstrate that in the study region, gravity modelling is a more easily controlled process than magnetic modelling due to high amount of remanent magnetization, the parameters of which vary locally and are mostly only known on a general level. However, lithological units also show petrophysical heterogeneity, and changes in metamorphic grade, in particular, can significantly affect the densities within a certain rock class; in order to understand the density distributions, it is also necessary to include a spatial aspect in the petrophysical data classification and analysis. Modelling examples show that with the careful application of geological and geophysical constraints, potential field modelling can detect sources at depths of several kilometres.

Keywords: geophysical methods, potential field, gravity methods, magnetic methods, petrophysics, density, magnetic properties, numerical models, Outokumpu

*Geological Survey of Finland, P.O. Box 96, FI-02151 Espoo, Finland*

*E-mail: hanna.levaniemi@gtk.fi*

## INTRODUCTION

Geophysical modelling and inversion is by nature ambiguous: for any given observed dataset, there are countless combinations of source geometries and properties that result in the observed anomalies. Thus, in order to produce geologically realistic models from geophysical data, knowledge of the dimensions and geometries of geological formations, and also their physical properties, is crucial for delimiting the degrees of freedom and for constraining and guiding the modelling towards the most realistic solution.

This study aims at discovering suitable model constraints, modelling parameter values and modelling methods in order to extend the detection depth ranges of potential field models (with emphasis on gravity data) for the Outokumpu Belt and its surroundings (Fig. 1). The first part of the study focuses on re-evaluating the existing petrophysical outcrop and drill core sample data. In the second part the petrophysical data is applied to modelling and inversion to study the potential for gravity and magnetic models to detect anomaly sources of different dimensions and at various depths.

An essential aspect in potential field modelling is the use of realistic petrophysical parameter values. Most recent petrophysical study in the Outokumpu region is the paper by Airo et al. (2011) that presents the petrophysical data from the Outokumpu Deep Drill Hole core samples. Petrophysical modelling parameter values "typical of the region" are listed in several reports, but they show some variation (Ahokas 1984, Ketola 1973, Ketola 1974, Ruotoistenmäki & Tervo 2006, Pekkarinen & Rekola 1994), most likely reflecting the modelling purposes and increase in the amount of data and regional coverage during the decades of exploration. The two previous comprehensive key documentations concentrating on petrophysical data are the detailed statistical approach of Lehtonen (1981), which uses lithological classification as a starting point, and the study by Ruotoistenmäki & Tervo (2006) based on petrophysical clustering. Although both of these works offer useful insights into the physical properties of the rocks in the study region, the statistical analysis according to rock classes of Lehtonen (1981) is the closer of these two to the purpose of this study. However, since Lehtonen's work, more data and also knowledge of the spatial variation in the properties has become available, and it is therefore appropriate at this point to update and complement his work.

Several extensive geological studies have been published in the Outokumpu region (e.g. Gaál et al. 1975, Koistinen 1981, Kontinen et al. 2006), but, although potential field data have been collected and modelled for the Outokumpu Belt throughout its exploration history, the previously documented modelling cases appear mostly scattered in various reports and unpublished papers. Ketola (1979) summarized the geophysical studies of the time on the Vuonos and Saramäki deposits: potential field modelling played an important role in exploration by Outokumpu Oy, albeit more as an indirect exploration tool. The gravimetric modelling that revealed the existence of the deep-plunging extension of the Outokumpu Belt between Vuonos and Kylylahti ("Papan putki") is extensively covered by Ahokas (1984) and discussed by Rekola & Hattula (1995) and Outokumpu News (1982).

The potential field datasets used in the examples of this study comprise ground gravity and magnetic data (by Outokumpu Oy) and various regional datasets. Four new gravimetric profiles were also measured as part of this study to complement the existing ground datasets.

Several reflection seismic profiles have been acquired in the study region during 2002-2008 in the FIRE and HIRE projects (Kukkonen & Lahtinen 2006, Kukkonen et al. 2011, Kukkonen et al. 2012). These seismic profiles provide a natural starting point for potential field modelling of deep-set sources. We discuss the possibilities and challenges on forward modelling of gravity data along the extended V7 and V8 seismic profiles. Deposit-scale modelling examples examine the application of the determined petrophysical parameters at the ends of the Outokumpu Belt, the Keretti and Kylylahti mining sites. The source detection depth range for gravity modelling is investigated with a synthetic example similar to the Kylylahti formation.

## GEOLOGICAL SETTING

The Outokumpu Belt, part of the Northern Karelian Schist Belt (NKSB), is located in Eastern Finland, close to the suture between the Archean gneissic-granitoid basement domain in the northeast and the Palaeoproterozoic Svecofennian domain in the southwest (Fig. 1). The Outokumpu area within the NSKB has been one of the most important mining districts in Finland, the main target having been the Outokumpu-type semi-massive–massive Co-Cu-Zn sulphides. The sulphide ores are hosted by the "Outokumpu assemblage" or "Outokumpu association" rocks, a rock assemblage comprising carbonate, skarn and quartz rocks appearing as folded and faulted fringes to massive serpentinised peridotite bodies (Gaál et al. 1975, Gaál & Parkkinen 1993, Peltonen et al. 2008). The Outokumpu assemblage rocks are hosted by allochthonous, metaturbiditic Kaleva greywackes ("mica schists") with intercalations of graphitic shales ("black schists"), in a nappe complex that rests upon the Archean gneiss granitoid basement. A sheet of Jatulian quartzites and arkoses occurs northwest of the Miihkali area in between the Archean basement and overlying Kalevian strata. The quartzite sheet is intruded by

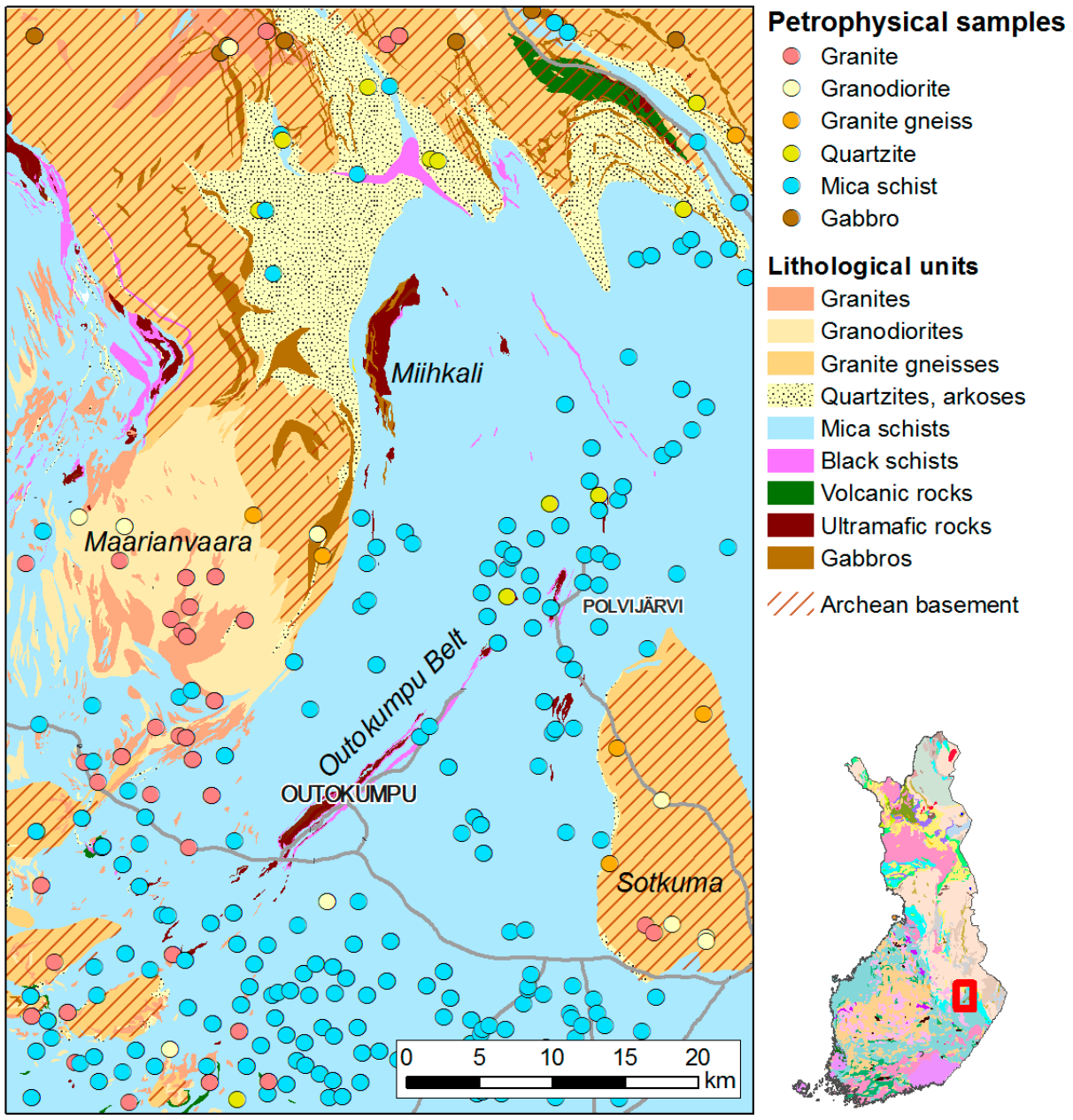


Fig. 1. Generalised bedrock map of the Outokumpu region. Modified from Bedrock of Finland – DigiKP. Contains data from the National Land Survey of Finland Topographic Database 03/2013.

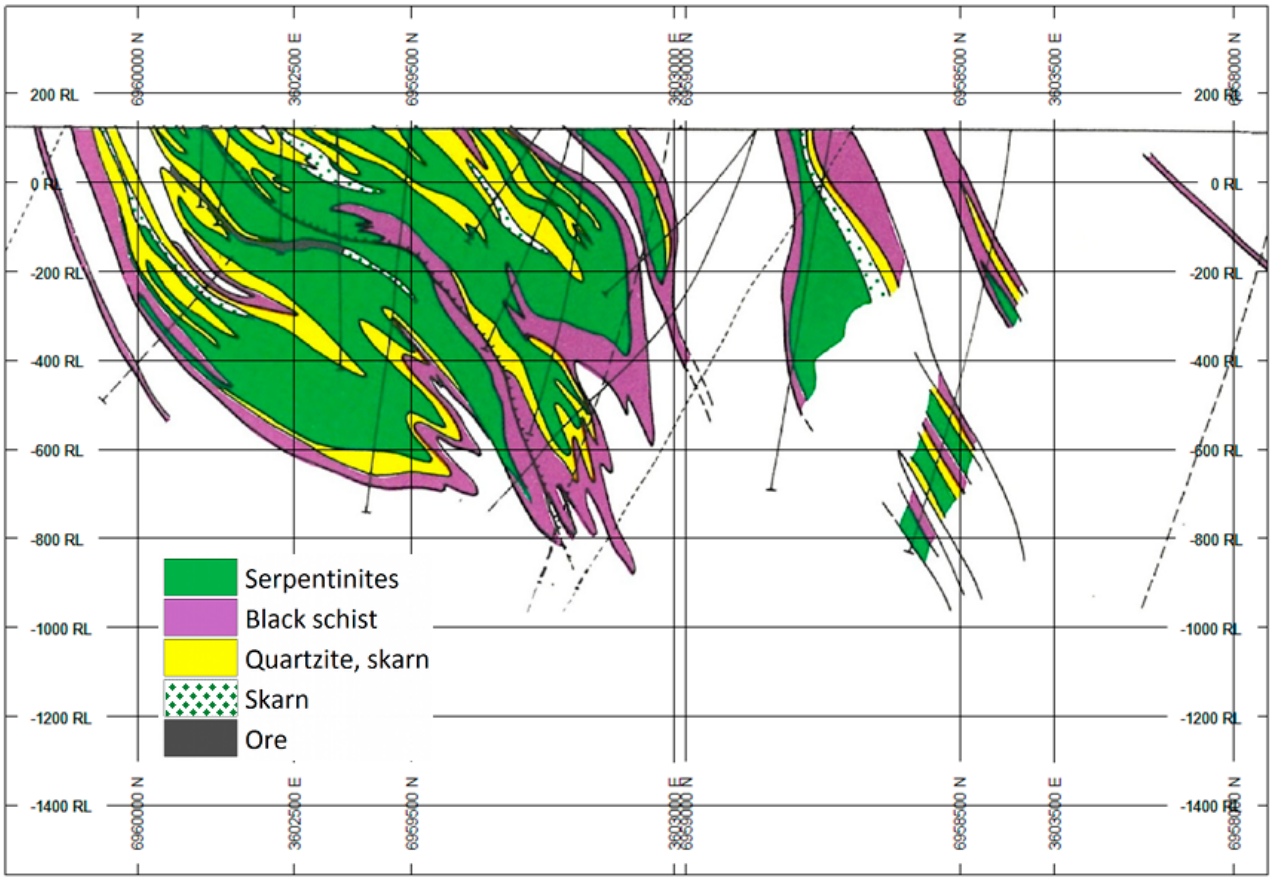


Fig. 2. Outokumpu geological section 186.630 (from Koistinen 1981).

ultramafic-mafic sills up to hundreds of metres thick that are also common in the Archean basement close to the Jatuli-Archean interface. West of the Outokumpu Belt, the Archean basement is intruded by the 1.86 Ga Maarianvaara granitoid suite. (Huhma 1971, Huhma 1986, Koistinen 1981, Peltonen et al. 2008, Kontinen et al. 2006).

The cross-section for profile 186.630 (Koistinen 1981) across the Outokumpu rock assemblage at the Outokumpu mine presented in Figure 2 illustrates a local geological set-up typical of the Outokumpu Belt: the meta-ultramafic massif, here mainly comprising serpentinised peridotite, quartz rocks and carbonate-skarn rocks, reaches the depth of several hundreds of metres, and with some variation extends along its northeast-bound strike for tens of kilometres. The carbonate, skarn and quartz rocks flank the folded serpentinite body (originally a thin, wide sheet (Koistinen 1981)) as thin fringes; all the presently known Outokumpu-type sulphide deposits are found in association with the fringing carbonate-skarn-quartz rock assemblage (Peltonen et al. 2008 and references therein). The black schists envelope the ultramafic rocks, and outside the Outokumpu assemblage rocks also appear as layers in the mica schist. The ultramafic bodies may also contain deformed and metamorphosed mafic rocks, mainly as small stocks, sills or dykes (Peltonen et al. 2008).

## DESCRIPTION OF DATASETS

### Petrophysical data

In this study we use petrophysical data from two sources: the regional GTK petrophysical database and the petrophysical data from drill core samples. The sparsely sampled GTK regional petrophysical database lacks data from the Outokumpu association rock types, but contains samples from all surrounding lithologies listed in Figure 1 except the volcanic and ultramafic rocks and black schists.

Thus it is ideal for characterizing the physical properties of regional lithological units. As the Outokumpu Belt has been quite thoroughly covered by drilling, for the Outokumpu association rock types, petrophysical cognizance can be augmented with analysis of the petrophysical samples from the drill cores, mainly produced by mining companies.

#### GTK database

The regional petrophysical database of Geological Survey of Finland (GTK) (Airo & Säävuori 2013) currently contains petrophysical data on more than 130,000 outcrop samples systematically collected over the whole country. The database entries contain location coordinates, rock class attributes and determinations of density, magnetic susceptibility and intensity of remanent magnetization. Petrophysical sampling methods, data acquisition and measurement equipment are described in Airo & Säävuori (2013). In the study region, the data selected for analysis amount to 591 samples (Fig. 1). The selection only includes samples that could be properly assigned to one of the lithological units in Figure 1 based on their rock class.

#### Petrophysical samples from drill cores

The Outokumpu Belt has been extensively drilled during the decades of exploration. In this study, three different data sources for petrophysical data from drill cores could be specified:

1. The GEOMEX project (Kontinen et al. 2006, Peltonen et al. 2008) assembled a database comprising historic drill core data from the Outokumpu Oy archives, as well as a few drill cores acquired during the GEOMEX project. For a significant number of the drill holes, petrophysical data (magnetic susceptibility, density and galvanic resistivity) are also available: within the GEOMEX project, the petrophysical data were addressed by Ruotoistenmäki & Tervo (2006).
2. Petrophysical drill core sample data from the Horsmanaho talc mine and its surroundings (Alava, Pehmytkivi and Karnukka sites), courtesy of Mondo Minerals B.V. (Pasi Talvitie, pers. comm. 2014).
3. Petrophysical drill core sample data from the Kylylahti Cu-Au-Zn mine site, courtesy of Boliden Kylylahti (Jari Juurela, pers. comm. 2015).

The data selected for analysis amount to ca. 38,000 density and 26,000 magnetic susceptibility samples.

In order to manage large amounts of data in a reasonable and meaningful way for modelling purposes, two questions must be considered: what is the suitable lithological classification and scale for analysing the data, and what are the factors affecting the value distributions within the selected lithological classification scheme?

The selected drill core data contains hundreds of distinct rock unit names ("field names") that make the classification of samples according to rock type an arduous task. For this reason, this study adapted the classification of the rock unit names used by Outokumpu Oy provided by the GEOMEX team in their assembled drill-core database. The data in the two other mining site databases were reclassified according to the GEOMEX convention. The classification was further narrowed down to seven key classes as per the typical geological setting (Fig. 2), each of which, for the

Table 1. Rock classes adopted from the GEOMEX project.

| General class | Class name | Abbreviation | Description |
|---|---|---|---|
| Outokumpu assemblage / Rocks of ultramafic origin | Serpentinites | SP | Serpentinised peridotites |
| | Talc-carbonate rocks (soapstones) | SS | Over 90% of carbonate and talc |
| | Other Outokumpu assemblage rocks of ultramafic origin | OUM | Carbonate rocks, skarns and quartz rocks |
| Outokumpu assemblage / other rocks | Outokumpu metabasites | OBA | Metamorphosed mafic rocks: gabbros, amphibolites and chlorite schists |
| | Sulphide mineralizations | SUL | Semi-massive to massive mineralizations |
| Schists (sedimentary origin) | Mica schists | MCS | Meta-greywackes |
| | Black schists | BS | Black schists |

purposes of potential field modelling, form a single modelling unit. The seven classes and their abbreviation used throughout this study are presented in Table 1.

The rocks within the rock classes presented in Table 1 show variation in mineral composition largely due to an increase in the metamorphic grade from a low amphibolite facies grade in the east to a high amphibolite facies grade in the west. Additional variables such as the local redox conditions and intensity of retrograde alteration also affect the variation, with all of these particularly affecting the serpentinites, but also calc-silicates and the hosting metasediments (Säntti et al. 2006). Thus, the region and accordingly the petrophysical databases should be further divided based on metamorphic zoning.

Figure 3 illustrates the locations and spatial division of the drill holes with petrophysical samples in the GEOMEX database, together with the metamorphic zoning. For serpentinites, antigorite and carbonate-antigorite serpentinites are most abundant in the east (zone A in Fig. 3), whereas the serpentinites in the west (zones B and C) are mainly mesh-textured lizardite-chrysotile serpentinites, in B zone dominantly derived from talc-olivine and anthophyllite olivine rocks and in zone C from anthophyllite and enstatite-anthophyllite rocks. Talc-carbonate rocks (soapstones) are restricted to zone A, there flanking the antigorite serpentinites. In zones B and C no prograde talc-carbonate rocks occur but retrograde talc-schists are met in late thin shear/fault zones dissecting serpentinites and skarn rocks. (Säntti et al. 2006)

In this study, the GEOMEX database was divided into five regional groups (Fig. 3): the Keretti group comprises the drill holes in Zone C, zone B is divided into the Vuonos group (in the Outokumpu Belt) and Miihkali group in the north, and in Zone A the database is divided into Horsmanaho and Kylylahti groups. Zone A also includes the Horsmanaho and Kylylahti mine site datasets.

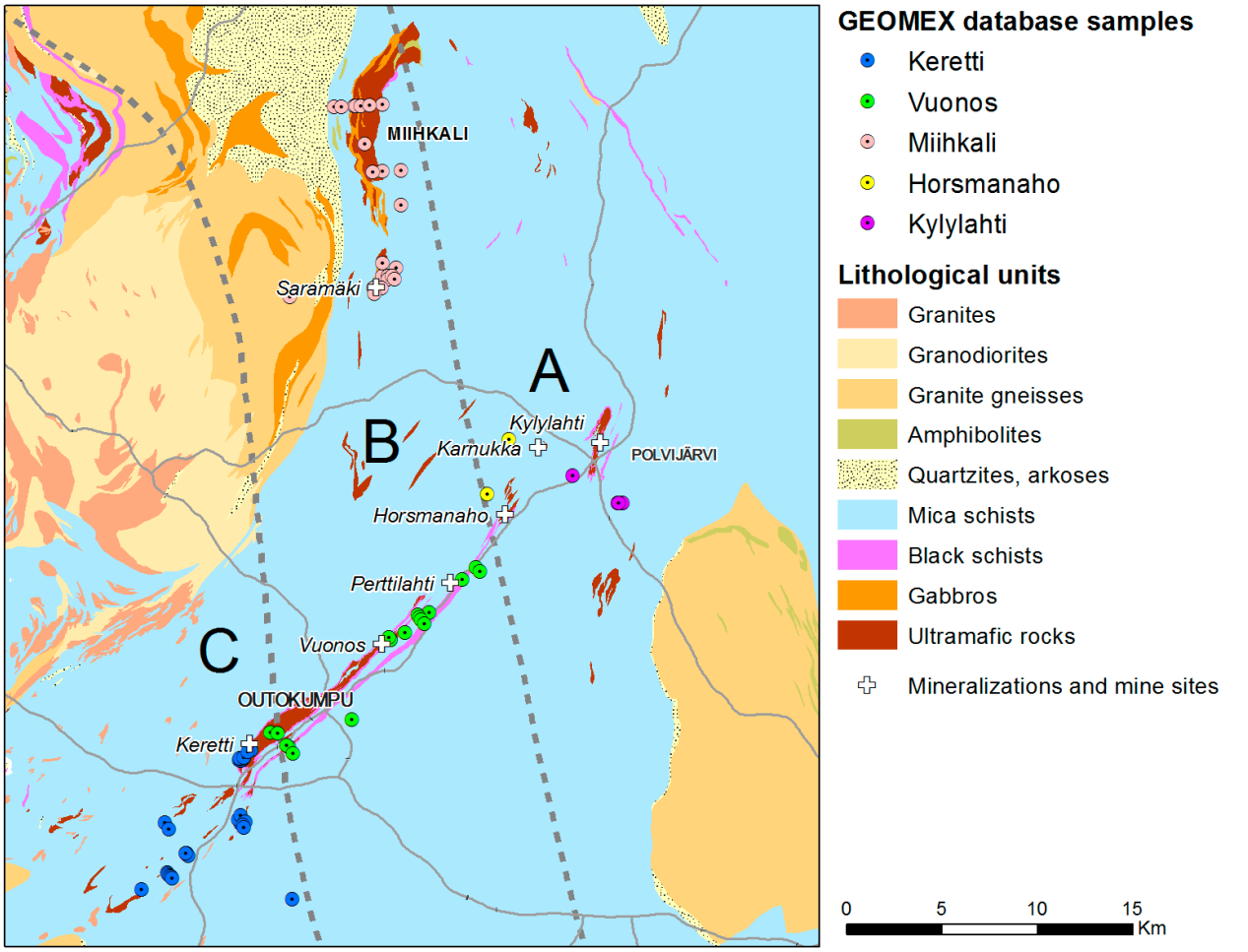


Fig. 3. Sites for the drill cores with petrophysical sampling and the metamorphic zones A, B and C (after Säntti et al. 2006). Bedrock map modified from Bedrock of Finland – DigiKP. Contains data from the National Land Survey of Finland Topographic Database 03/2013.

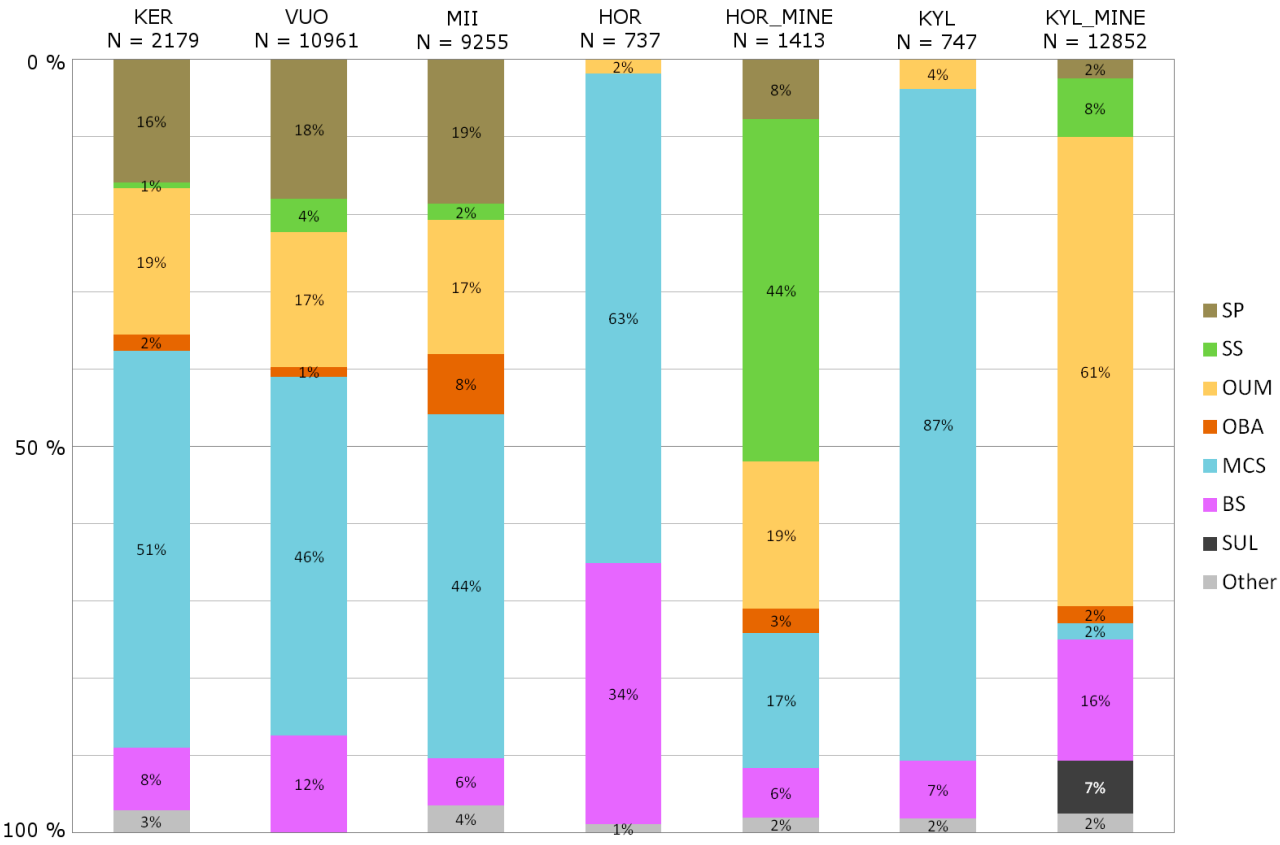


Fig. 4. Internal rock-class distributions of density samples within each data group. KER = Keretti (GEOMEX), VUO = Vuonos (GEOMEX), MII = Miihkali (GEOMEX), HOR = Horsmanaho (GEOMEX), HOR_MINE = Horsmanaho (mine site), KYL = Kylylahti (GEOMEX), KYL_MINE = Kylylahti (mine site). For rock class descriptions, see Table 2.

As emphasised by Ruotoistenmäki & Tervo (2006), all available drill-core data originate from various exploration projects and as such do not provide an objective view of the geological setting, but are biased towards certain rock types or, independently of the rock type, may be abnormally enriched in disseminated sulphides. The rock class distributions from samples with density measurements for each drill-hole data group are presented in Figure 4. The serpentinites (SP) are most abundant in the westernmost zones (Keretti–Miihkali–Vuonos). Talc-carbonate rocks (SS) are most dominantly present in the data from the Horsmanaho mining site, but the distribution also depicts the relative scarcity of soapstones in the west (see text related to Fig. 3). The Kylylahti mine data emphasise the Outokumpu altered ultramafic rock class (OUM), which hosts the sulphide mineralization. The GEOMEX database drill holes in Horsmanaho and Kylylahti mainly consist of mica schists and enclosed black schist layers.

## Potential field datasets

Both ground gravity and magnetic data (by Outokumpu Oy) exist for the study region and for the most part cover the Outokumpu Belt and Miihkali massif formations (Fig. 5). The vertical component gravity data were mostly collected with 100-m line spacing and 20-m sample spacing, and the vertical component magnetic data with 50-m line spacing and 10-m sample spacing.

In addition to local ground surveys, the study region is mostly covered by more sparsely sampled regional gravity data (Elo 2003) with mostly dispersed sample locations and ca. 500–1000 m sample spacing, the 5 x 5 km gravity grid of the Finnish Geospatial Research Institute FGI (Kääriäinen & Mäkinen 1997) and airborne magnetic data of GTK (Hautaniemi et al. 2005). The regional gravity datasets are used and referred to, together with local data, in the modelling examples.

Several reflection seismic profiles have been acquired in the study region during 2002–2008 in

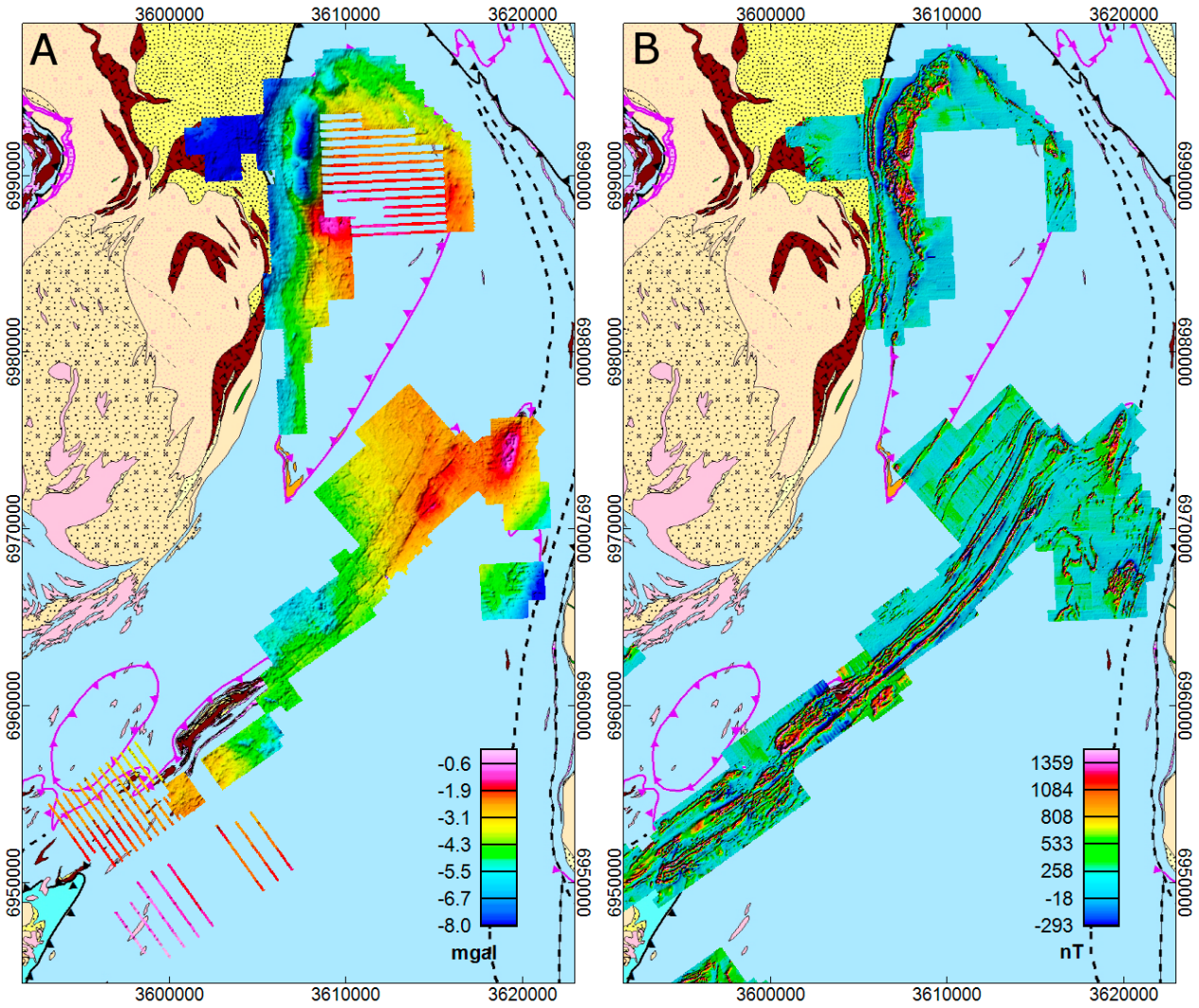


Fig. 5. Ground gravity (A) and magnetic (B) surveys in the Outokumpu–Miihkali region. Bedrock map: Bedrock of Finland – DigiKP.

the FIRE and HIRE projects (Kukkonen & Lahtinen 2006, Kukkonen et al. 2011, and Kukkonen et al. 2012). The profile locations are shown in Figure 6. One aim of this study is to model the deep-set features accross the Outokumpu region, and the existing seismic profiles provide a natural starting point for potential field modelling. However, as the existing detailed potential field datasets were found to cover the Outokumpu Belt rather narrowly (Fig. 5), in order to complement the data on the reflection seismic profiles and in other regions lacking coverage, new gravity profiles were measured as part of this study along local roads with 50-m sample spacing in 2014 (Fig. 6).

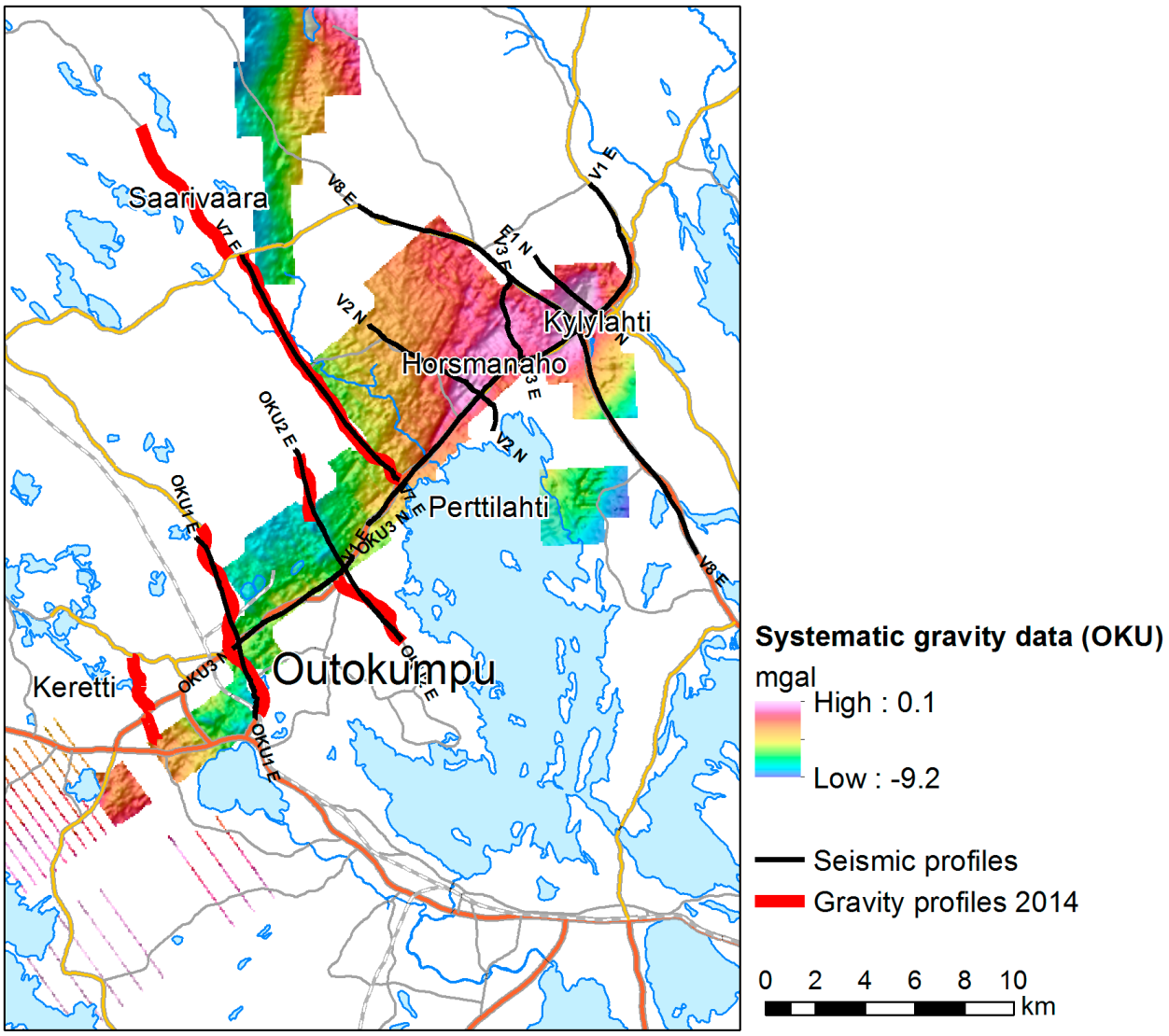


Fig. 6. New gravimetric profile locations. Contains data from the National Land Survey of Finland Topographic Database 03/2013.

## PETROPHYSICAL DATA ANALYSIS

### GTK database

The density-susceptibility diagram for the rock classes in the GTK database is presented in Figure 7 and the characterizing density statistics in Table 2. The granites (mostly from the Maarianvaara batholith) have the lowest densities, with a median of ca. 2600 kg/m$^3$, although the medians of granodiorites and quartzites are quite close (2622 and 2635 kg/m$^3$, respectively). The granite gneisses (2666 kg/m$^3$) dominating the Archean basement complex are lighter than the mica schists in the overlying Kaleva package (2704 kg/m$^3$). Gabbroic rocks in the ultramafic-mafic sills along the Archaean-Proterozoic interface expectedly have the highest densities, with the median value of 2985 kg/m$^3$.

The susceptibilities of the samples mainly remain in the paramagnetic population (values below 2000 µSI as defined by Airo & Säävuori 2013). The only rock class with clearly ferrimagnetic samples is the gabbro class, indicating the presence of magnetite-rich, high-density gabbros in the region. Some granites also have high magnetic susceptibilities.

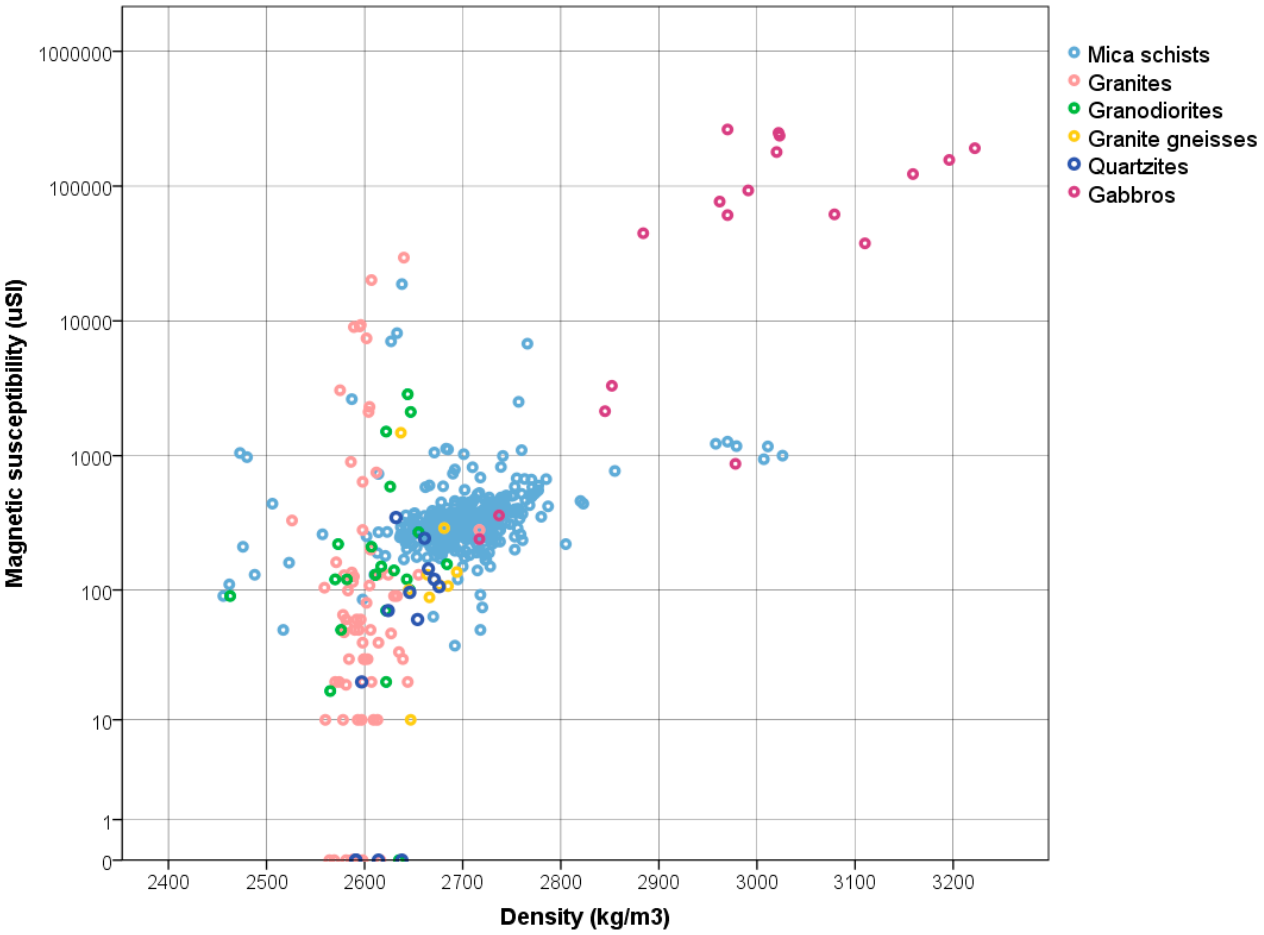


Fig. 7. Density–susceptibility diagram for the rock classes in the GTK database.

Table 2. Descriptive density statistics for the rock classes in the GTK database.

| Rock class | N | Mean (kg/m³) | Median (kg/m³) | Standard deviation (kg/m³) |
|---|---|---|---|---|
| Granites | 77 | 2598 | 2596 | 25 |
| Granodiorites | 23 | 2610 | 2622 | 44 |
| Granite gneisses | 9 | 2666 | 2666 | 20 |
| Quartzites | 14 | 2625 | 2635 | 48 |
| Mica schists | 450 | 2702 | 2704 | 58 |
| Gabbros | 18 | 2985 | 2985 | 142 |
| Total | 591 | | | |

## Drill-core data

### Density distributions

Density distributions and statistical key figures for each group are presented in Figure 8 and Table 3. The serpentinite (SP) densities clearly reflect the metamorphic zonation; the chrysotile serpentinites in the west are on average notably lighter than the antigorite serpentinites in the east. This difference was also noted on a general level by Lehtonen (1981). The talc-carbonate rocks (SS), which are in fact restricted to zone A in Figure 3, have a median density of 2908 kg/m³ in Horsmanaho, where this rock type is most abundantly present in the data; in the west, the rocks labelled as talc-carbonate rocks are most likely shear-related talc schists (A. Kontinen, pers. comm. 2015). The other rocks of ultramafic origin (OUM) show a wider range of values, but the value distributions are quite similar to the median values, ranging around 2800–2900 kg/m³. Metabasites (OBA) are mostly

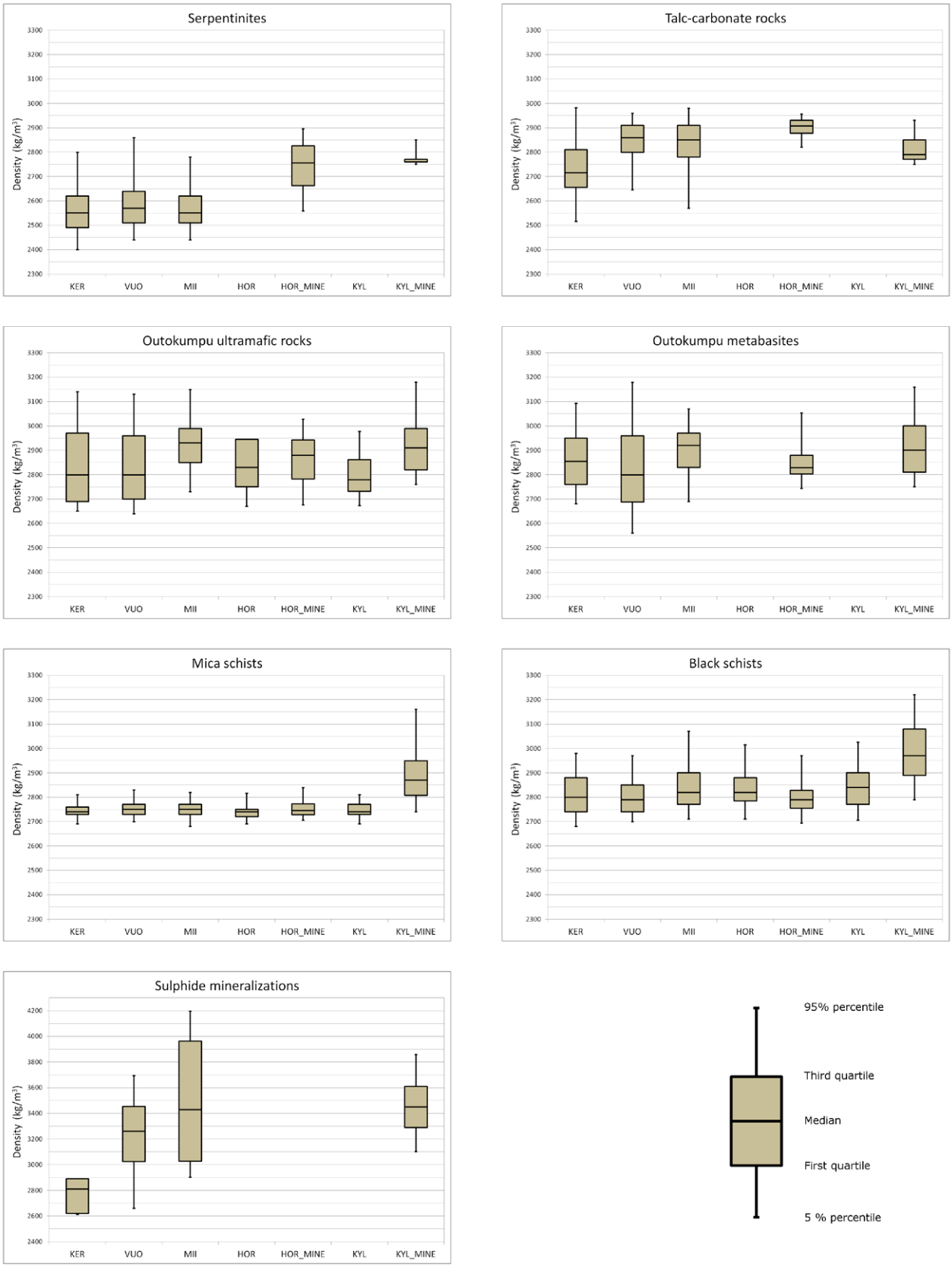


Fig. 8. Density distributions for each Outokumpu Belt rock type according to region (KER = Keretti (GEOMEX), VUO = Vuonos (GEOMEX), MII = Miihkali (GEOMEX), HOR = Horsmanaho (GEOMEX), HOR_MINE = Horsmanaho (mine site), KYL = Kylylahti (GEOMEX), KYL_MINE = Kylylahti (mine site). The vertical scale for the sulphide mineralization class differs from the rest of the diagrams. (Note: not all groups have samples from all rock classes).

Table 3. Density statistics according to rock class for each drill-hole group. For rock classes, see Table 1. For groups, see Figures 3 and 4. Q1 = first quartile, Q3 = third quartile. The unit for values is kg/m$^3$. (Note: not all groups have samples from all rock classes). KER = Keretti (GEOMEX), VUO = Vuonos (GEOMEX), MII = Miihkali (GEOMEX), HOR = Horsmanaho (GEOMEX), HOR_MINE = Horsmanaho (mine site), KYL = Kylylahti (GEOMEX), KYL_MINE = Kylylahti (mine site).

| ROCK CLASS | GROUP | N | Mean | Q1 | Median | Q3 | Std.dev. |
|---|---|---|---|---|---|---|---|
| | KER | 820 | 2568 | 2490 | 2550 | 2620 | 123 |
| | VUO | 1963 | 2598 | 2510 | 2570 | 2640 | 167 |
| | MII | 1721 | 2572 | 2510 | 2550 | 2620 | 106 |
| SP | HOR | | | | | | |
| | HOR_MINE | 109 | 2742 | 2662 | 2756 | 2826 | 104 |
| | KYL | | | | | | |
| | KYL_MINE | 313 | 2772 | 2760 | 2760 | 2770 | 66 |
| | KER | 42 | 2727 | 2655 | 2715 | 2810 | 131 |
| | VUO | 469 | 2843 | 2800 | 2860 | 2910 | 99 |
| | MII | 192 | 2825 | 2780 | 2850 | 2910 | 124 |
| SS | HOR | | | | | | |
| | HOR_MINE | 626 | 2901 | 2878 | 2908 | 2931 | 44 |
| | KYL | 2 | 2854 | 2838 | 2854 | | 22 |
| | KYL_MINE | 978 | 2811 | 2770 | 2790 | 2850 | 59 |
| | KER | 979 | 2842 | 2690 | 2800 | 2970 | 175 |
| | VUO | 1906 | 2837 | 2700 | 2800 | 2960 | 172 |
| | MII | 1603 | 2933 | 2850 | 2930 | 2990 | 144 |
| OUM | HOR | 13 | 2843 | 2750 | 2830 | 2945 | 113 |
| | HOR_MINE | 268 | 2869 | 2783 | 2880 | 2943 | 138 |
| | KYL | 28 | 2795 | 2732 | 2780 | 2862 | 85 |
| | KYL_MINE | 7802 | 2926 | 2820 | 2910 | 2990 | 136 |
| | KER | 106 | 2865 | 2760 | 2855 | 2950 | 133 |
| | VUO | 130 | 2829 | 2688 | 2800 | 2960 | 194 |
| | MII | 710 | 2900 | 2830 | 2920 | 2970 | 121 |
| OBA | HOR | | | | | | |
| | HOR_MINE | 45 | 2854 | 2804 | 2828 | 2880 | 83 |
| | KYL | | | | | | |
| | KYL_MINE | 284 | 2914 | 2810 | 2900 | 3000 | 133 |
| | KER | 2654 | 2747 | 2730 | 2740 | 2760 | 54 |
| | VUO | 5063 | 2757 | 2730 | 2750 | 2770 | 58 |
| | MII | 4102 | 2753 | 2730 | 2750 | 2770 | 62 |
| MCS | HOR | 467 | 2742 | 2720 | 2740 | 2750 | 42 |
| | HOR_MINE | 247 | 2754 | 2728 | 2745 | 2773 | 44 |
| | KYL | 648 | 2746 | 2730 | 2740 | 2770 | 41 |
| | KYL_MINE | 262 | 2894 | 2807 | 2870 | 2950 | 122 |
| | KER | 423 | 2819 | 2740 | 2800 | 2880 | 106 |
| | VUO | 1367 | 2804 | 2740 | 2790 | 2850 | 96 |
| | MII | 566 | 2850 | 2770 | 2820 | 2900 | 133 |
| BS | HOR | 249 | 2840 | 2785 | 2820 | 2880 | 96 |
| | HOR_MINE | 90 | 2799 | 2756 | 2790 | 2829 | 73 |
| | KYL | 55 | 2837 | 2770 | 2840 | 2900 | 97 |
| | KYL_MINE | 2018 | 2986 | 2890 | 2970 | 3080 | 135 |
| | KER | 7 | 2794 | 2620 | 2810 | 2890 | 140 |
| | VUO | 29 | 3210 | 3025 | 3260 | 3455 | 301 |
| | MII | 36 | 3494 | 3028 | 3430 | 3963 | 463 |
| SUL | HOR | | | | | | |
| | HOR_MINE | | | | | | |
| | KYL | | | | | | |
| | KYL_MINE | 882 | 3454 | 3290 | 3450 | 3610 | 230 |

relevant to the large Miihkali massif (see Fig. 4), and there have a median density of 2920 kg/m$^3$.

The density value distributions for mica schists are very uniform, with median values of 2740–2750 kg/m$^3$, although there is a spread from c. 2650 to 2780 kg/m$^3$. The median is slightly higher than the median value for the mica schists in the GTK regional database (Table 1), which probably reflects two factors: 1) the general enrichment of sulphides in the mica schists in drill cores from ore environments where mica schists often occur close and grade into sulphiditic black schists, and 2) the more weathered nature of the outcrops where the GTK samples have been collected (A. Kontinen, pers. comm. 2015). The black schists, heavier than the mica schists, also show more deviation in their densities. For both of the schist classes, the Kylylahti mine densities are notably higher than for the other datasets; Pekkarinen & Rekola (1994) also reported high densities for black schists, but as the GEOMEX database does not confirm the uncustomary increase in mica schist densities in Kylylahti, the reason for the high mica schist densities in the mine site database remains unclear.

The number of sulphide mineralization samples is generally very low, with the exception of the Kylylahti mine site dataset. Moreover, the sulphide mineralization grades in the samples vary from semi-massive to massive ore, which inevitably affects the density ranges. The most reliable (with regard to the number of samples) Kylylahti dataset has a median density of 3450 kg/m$^3$. Given the relatively low density of the Keretti samples, they most likely originate from the disseminated/veined type Co-Ni Hautalampi deposit parallel to the Keretti main ore (A. Kontinen, pers. comm. 2015).

### Magnetic susceptibility distributions

The GEOMEX magnetic susceptibility dataset proved to be more problematic than the density data, as it contains an abnormally large number of zero susceptibility values (18% of all data). Some of these values are without doubt true readings, but the high number of zero values leads to a suspicion that missing values have been transformed into zeroes sometime during the long life span of this dataset. Therefore, in this study, all the zero values were rejected from the statistical analysis. Given that this most likely also removed true readings, the statistics may be slightly biased towards larger ends of the value ranges. It should also be noted that some of the data may date back to a time when the measurement sensitivity for magnetic susceptibilities was not yet up to current standards, and this may affect the overall accuracy of the data analysis.

The magnetic susceptibility value distributions are often bi-peaked due to their paramagnetic and ferromagnetic components (e.g. Airo & Säävuori 2013), and as such are often best presented as value distribution histograms instead of statistical key figures. The histograms for magnetic susceptibilities according to the region and rock class are presented in Figure 9 (note: some groups have no or very few samples from a certain rock class; if the number of samples N < 15, no histogram is plotted). The two clear rock classes with moderately high magnetic susceptibilities are the (chrysotile) serpentinites (SP), due to their magnetite content, and the black schists (BS), due to their monoclinic pyrrhotite content. In general, according to the distributions, the magnetic susceptibility values of the serpentinites appear to decrease towards the east, mirroring the change from chrysotile serpentinites in the west to antigorite serpentinites in the east (Horsmanaho, Kylylahti). The black schist susceptibilities similarly decrease towards the east, reflecting either a decrease in the amount of pyrrhotite or the presence of hexagonal (antiferromagnetic) pyrrhotite, which has also been detected in the black schists of the Outokumpu region (Airo et al. 2011).

### Remanent magnetization

The GEOMEX database does not contain remanent magnetization measurements. According to Ahokas (1980), during 1974–1977, Outokumpu Oy performed measurements of remanent magnetization intensities and directions on an outcrop sample set mostly containing black schists, serpentinites and skarn rocks. However, due to the low number of samples and large spread of values, the results were not considered reliable except for the black schists: the remanence magnetization parameters in the Outokumpu and Miihkali regions are presented in Table 4.

The Horsmanaho mine site dataset contains determinations for the intensity of remanent magnetization, which enables calculation of the Koenigsberger ratio (Q), i.e. the ratio of remanent magnetization to induced magnetization (dependant on magnetic susceptibility $k$). The Q value indicates whether induced or remanent magnetization is more dominant in a given sample; for the

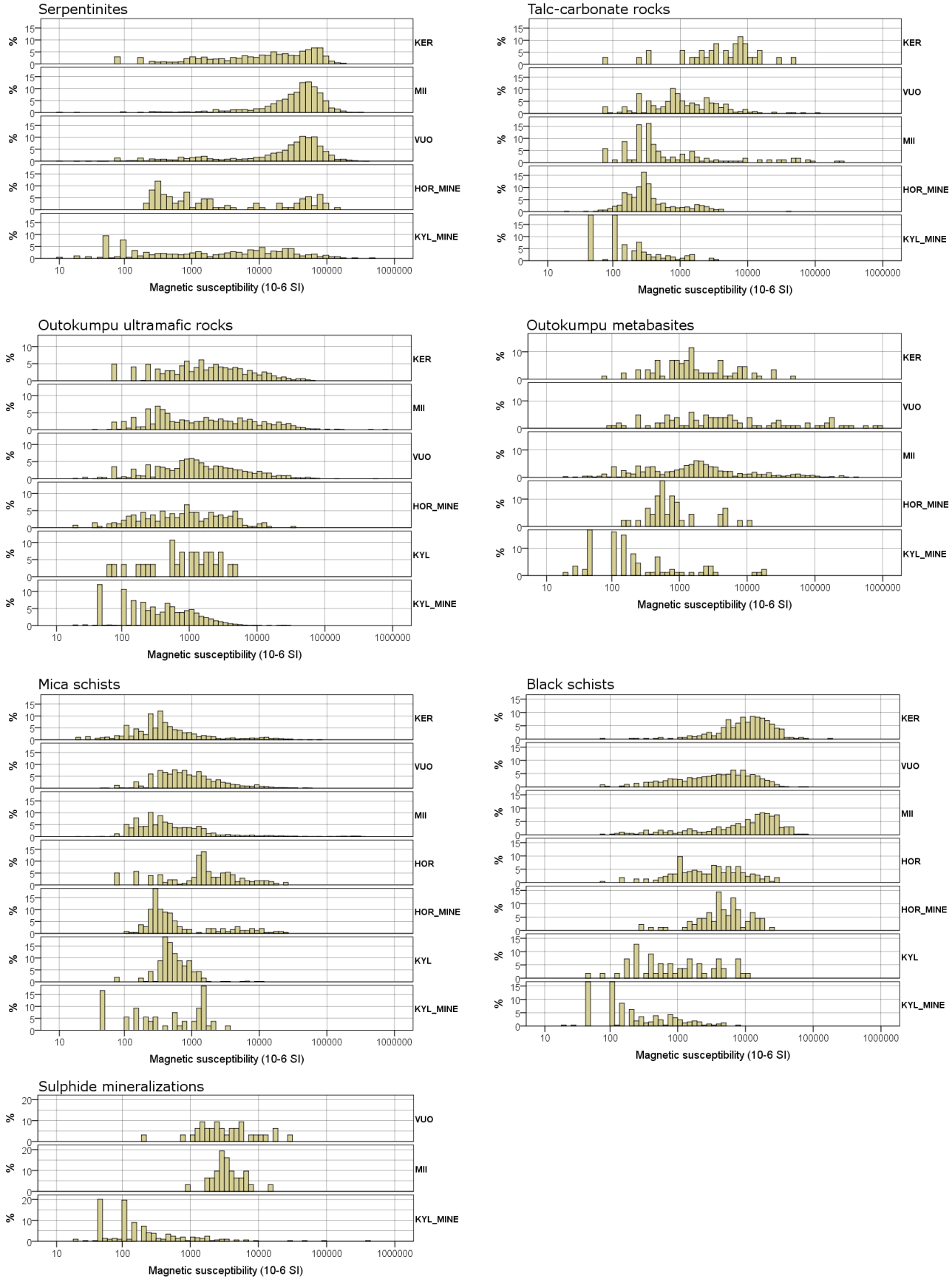


Fig. 9. Magnetic susceptibility histograms according to the rock class and region. KER = Keretti (GEOMEX), VUO = Vuonos (GEOMEX), MII = Miihkali (GEOMEX), HOR = Horsmanaho (GEOMEX), HOR_MINE = Horsmanaho (mine site), KYL = Kylylahti (GEOMEX), KYL_MINE = Kylylahti (mine site). For rock class descriptions, see Table 1.

Table 4. Remanent magnetization parameters for black schists (from Ahokas 1980).

| | Koenigsberger ratio (Q) | Inclination | Declination |
|---|---|---|---|
| Outokumpu Belt | 8 | 45° | 70° |
| Miihkali | 10 | 45° | 90° |

latter (Q > 1), modelling becomes more challenging if the direction of the remanent magnetization is not known (as is often the case). This is especially the case for small-grained pyrrhotite and magnetite, as they can better retain stable remanent magnetization directions that deviate from the current direction of the Earth's field (e.g. Clarke 1997).

In the Horsmanaho mine site dataset, for samples with moderate to high susceptibility ($k$ > 1000 μSI), there are numerous Q values of 10–100, most notably for the black schists (for other rock classes, the majority of the samples belong to the $k$ < 1000 μSI population; see Fig. 9). This conforms to or, in fact, exceeds the findings of Outokumpu Oy discussed above, indicating that especially for black schists, remanent magnetization plays a prominent role as the magnetic anomaly source. For serpentinites, Q reaches values of 1–5, but the dominant direction of remanent magnetization, if exists, remains unknown.

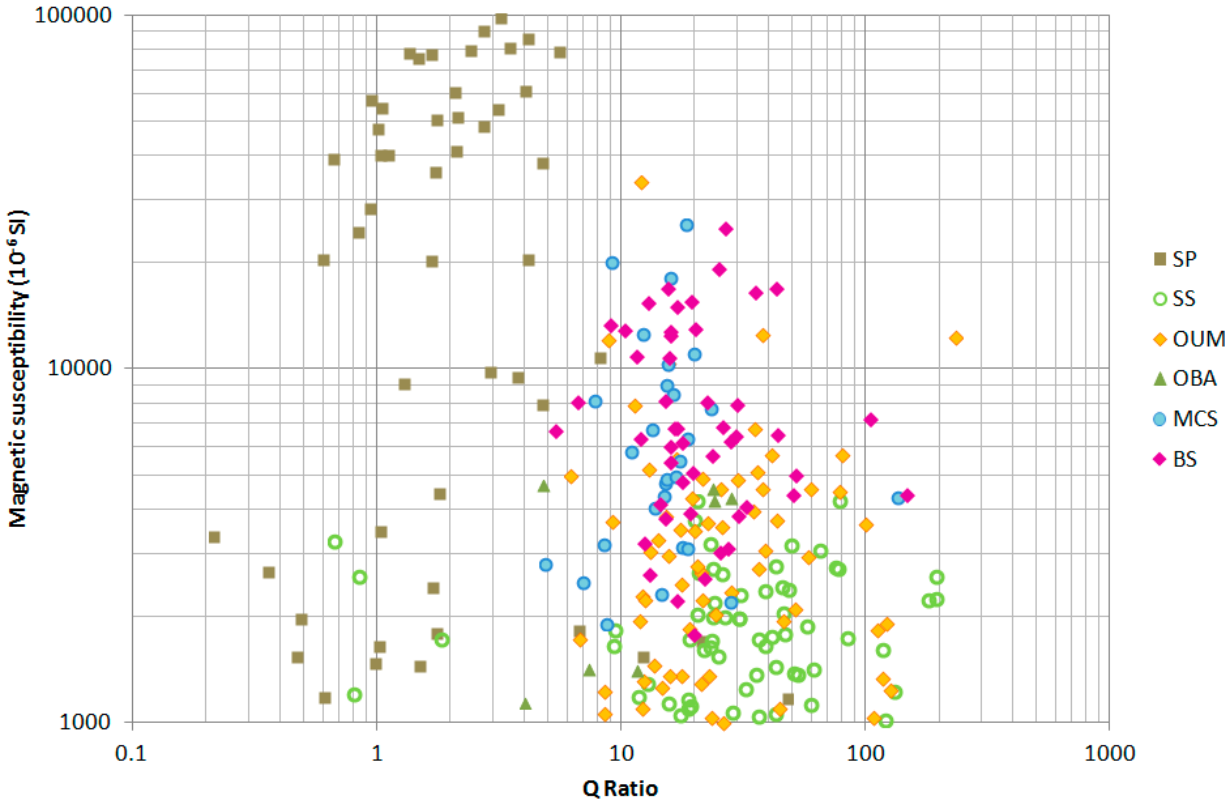


Fig. 10. Magnetic susceptibility ($k$) versus Q ratio diagram for the Horsmanaho mine site dataset for samples with $k$ > 1000 μSI. Data courtesy of Mondo Minerals B.V. For rock class descriptions, see Table 1.

## MODELLING EXAMPLES

The following chapters present both regional-scale (along the extended V7 and V8 seismic profiles) as well as the deposit-scale (the Keretti profile and the Kylylahti deposit) modelling examples. Modelling of the Miihkali massif north of the Outokumpu Belt is presented by Lahti et al. (2016, this volume) and the V7 example is discussed in a more extensive context by Heinonen et al. (2016, this volume).

## Regional modelling of seismic profiles V7 and V8

To study the deep-set features across the Outokumpu region, the gravity data were forward modelled along the extended V7 and V8 seismic profiles (Kukkonen & Lahtinen 2006) (Fig. 11). The modelling was performed with Tensor Research ModelVision 14.1 software.

For the V7 profile, the gravity modelling data consist of the new 2014 profile data (Fig. 6 and related text). For the profile V8, the data were sampled from the interpolated regional gravity data (Elo 2003), and outside the regional data coverage the values were estimated based on the interpolated raster of the 5 x 5 km national data grid courtesy of the Finnish Geospatial Research Institute FGI (Kääriäinen & Mäkinen 1997).

The seismic section images of the profiles V7 and V8 show strong reflectors at the depths of one kilometre and below. These are similar to the strong upper-crust reflector on FIRE-3 pierced by the Outokumpu Deep Drill Hole; the reflective response there was confirmed to originate from Outokumpu assemblage rocks (Kukkonen 2011), and consequently, Kukkonen et al. (2012) discussed all the seismic profiles and the nature of strong reflectors in the region. For profile V7, instead of or at least in addition to possible Outokumpu assemblage rocks, the most likely source candidate for the strong, deep-plunging reflectors was discovered by Kontinen & Säävuori (2013), who documented a shallow two-hole drilling in Saarivaara, ca. 1 km NW of the northern end of V7 (Fig. 11). The data have since been augmented by two additional drill holes (Fig. 12). The drilling revealed a sequence of alternating layers of calc-silicate gneisses, metadiabases, Jatulian quartzites and Archean gneisses, and the strike and dip of the layers is well in accordance with the strong reflectors in the northwestern part of the V7 seismic section image. For profile V8, there are similar reflective features, and as the distance between the profiles is relatively small, it is assumed here that the same geological environment prevails in both profiles.

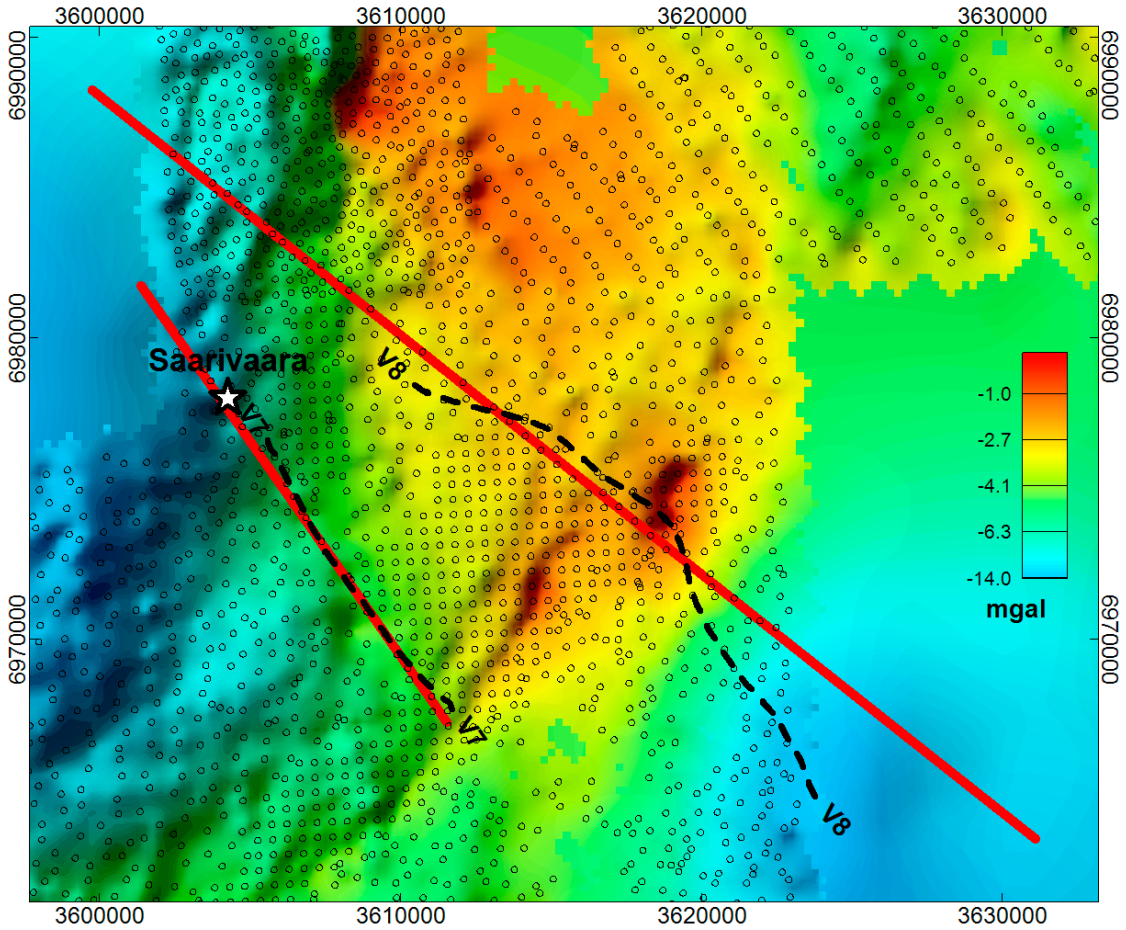


Fig. 11. Gravity modelling profile locations (in red) along the seismic lines V7 and V8 (in black). The sample coverage of the regional gravity data is marked by dot symbols. Outside the regional data coverage, the map displays FGI data.

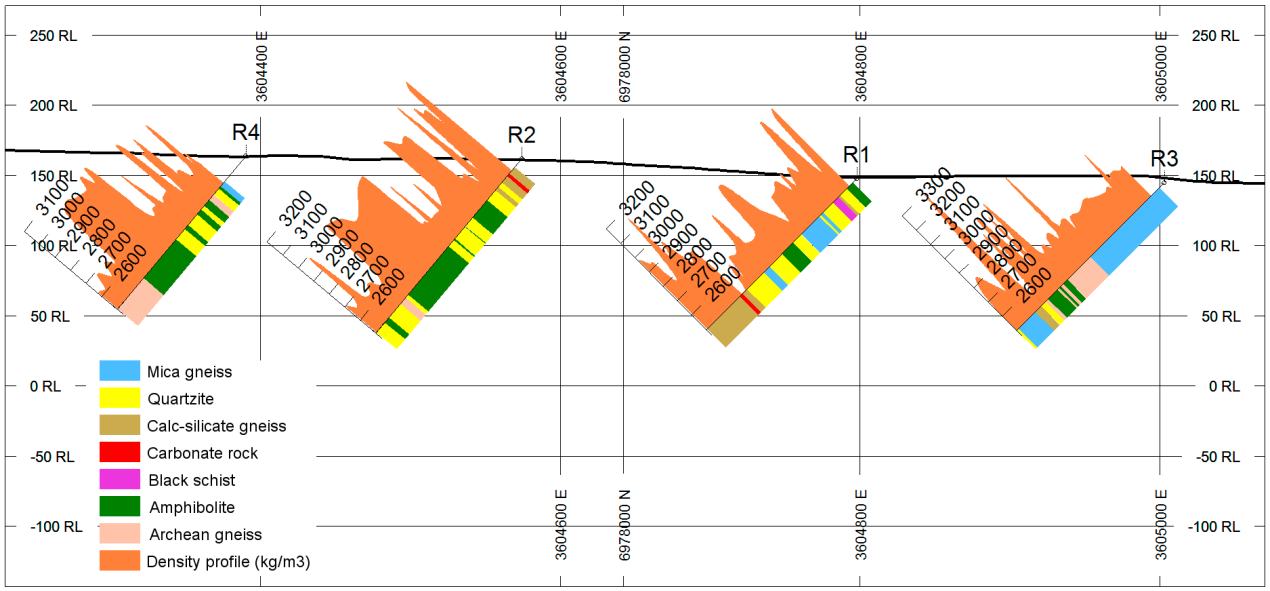


Fig. 12. Saarivaara drilling profile. Input data provided by A. Kontinen. Figure modified from Kontinen & Säävuori (2013).

Based on the drill core densities in the Saarivaara drilling profile, the density of quartzites and arkosites in the strata is ca. 2650 kg/m³, mica gneisses ca. 2750 kg/m³, calc-silicate gneisses ca. 2850–3150 kg/m³ and amphibolites 2950–3050 kg/m³. The unit of alternating layers is estimated to be 300–500 m thick and internally strongly foliated. Even more high-density amphibolites layers may exist within the underlying Archean gneisses, which would explain the considerable thickness of the reflectors. (Kontinen & Säävuori 2013)

The V7 profile is located on the metamorphic zone B (Fig. 3) and the V8 profile crosses from zone A to B. The strong upper-crust reflector on FIRE-3 related to Outokumpu assemblage rocks encountered at the depths of 1300–1500 m in the Outokumpu Deep Drill Hole (also on zone B, ca. 2 km east of the Outokumpu town) shows mean densities of ca. 2600 kg/m³ (serpentinites) to ca. 2900–3000 kg/m3 (skarns and black schists) (Airo et al. 2011). On zone B, in general, the median density of serpentinites is ca. 2550 g/cm3 and on zone A 2760 kg/m³. The density of the other altered ultramafic rocks varies approximately between 2800–2930 kg/m³ (Table 3).

The density ranges of both the Saarivaara reflector rocks and Outokumpu association rocks are wide and for any gravity model body, the overall density contrast with the host rock (mica schist) depends on the rock composition. With the many degrees of freedom present in interpretation models, the Outokumpu association rocks and Saarivaara type rocks could not be reliably separated from each other by their overall densities, even if some of the strong seismic reflectors were due to the Outokumpu association. In the model presented here, the estimated average density of 2800 kg/m³ is used for all reflective packages.

The modelling parameters on gravimetric profiles V7 and V8 are presented in Table 5. The V8 profile extends from the Maarianvaara granite in the northwest to the Archean Sotkuma gneiss in the southeast (Fig. 1, Fig. 11). On the gravimetric Bouguer anomaly map, granite and gneiss present as gravity minima due to the low density of the granitoids of ca. 2670 kg/m³ (Table 2). This value

Table 5. Gravity model parameters.

| | **Profile V7** | **Profile V8** |
|---|---|---|
| Gravity data source | GTK 2014 survey (projected on a straight profile) | Regional gravity data (APV); outside the APV survey region, FGI data were used |
| Model body extents / densities | Outokumpu allochthon metasediments: 20 km / 2720–2740 kg/m³<br>Saarivaara reflectors: 10 km / 2800 kg/m³<br>Outokumpu Belt (on V8): 5 km / 2800 kg/m³ | |
| Regional level | -13.0 mgal | |

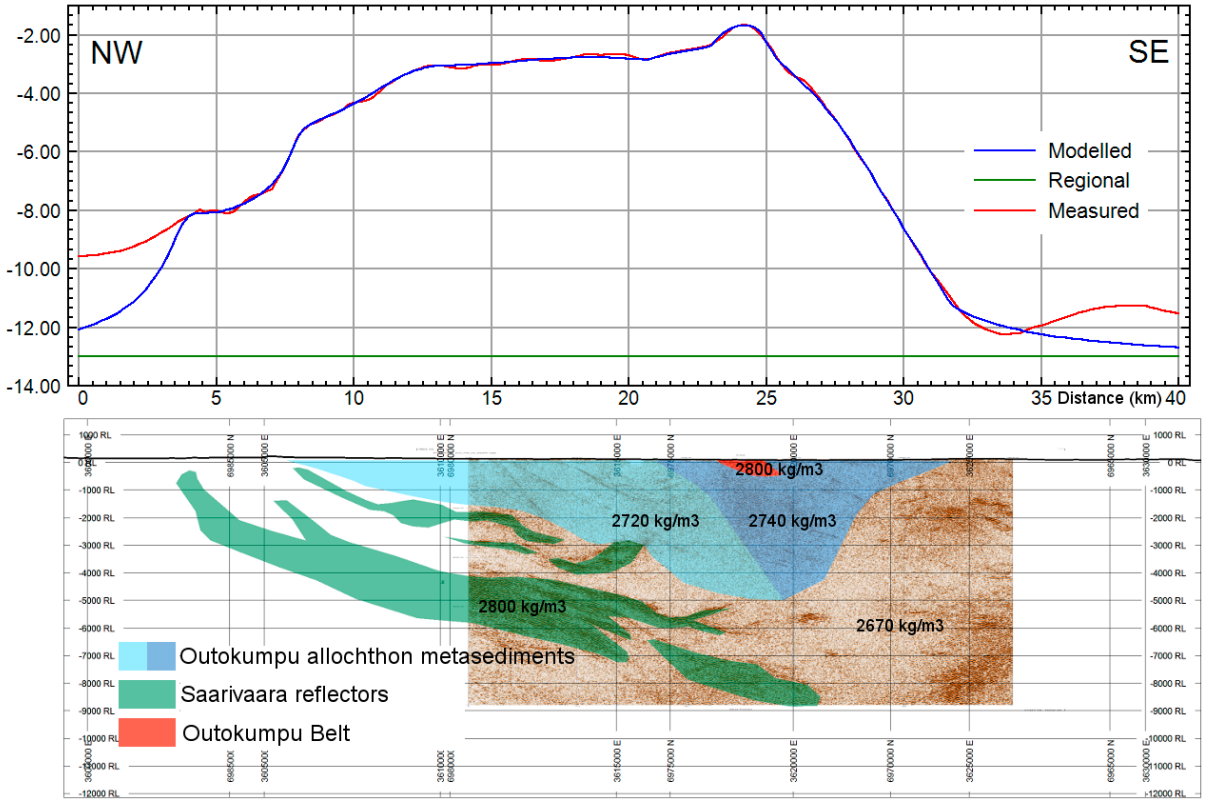


Fig. 13. Bouguer anomaly model along seismic profile V8.

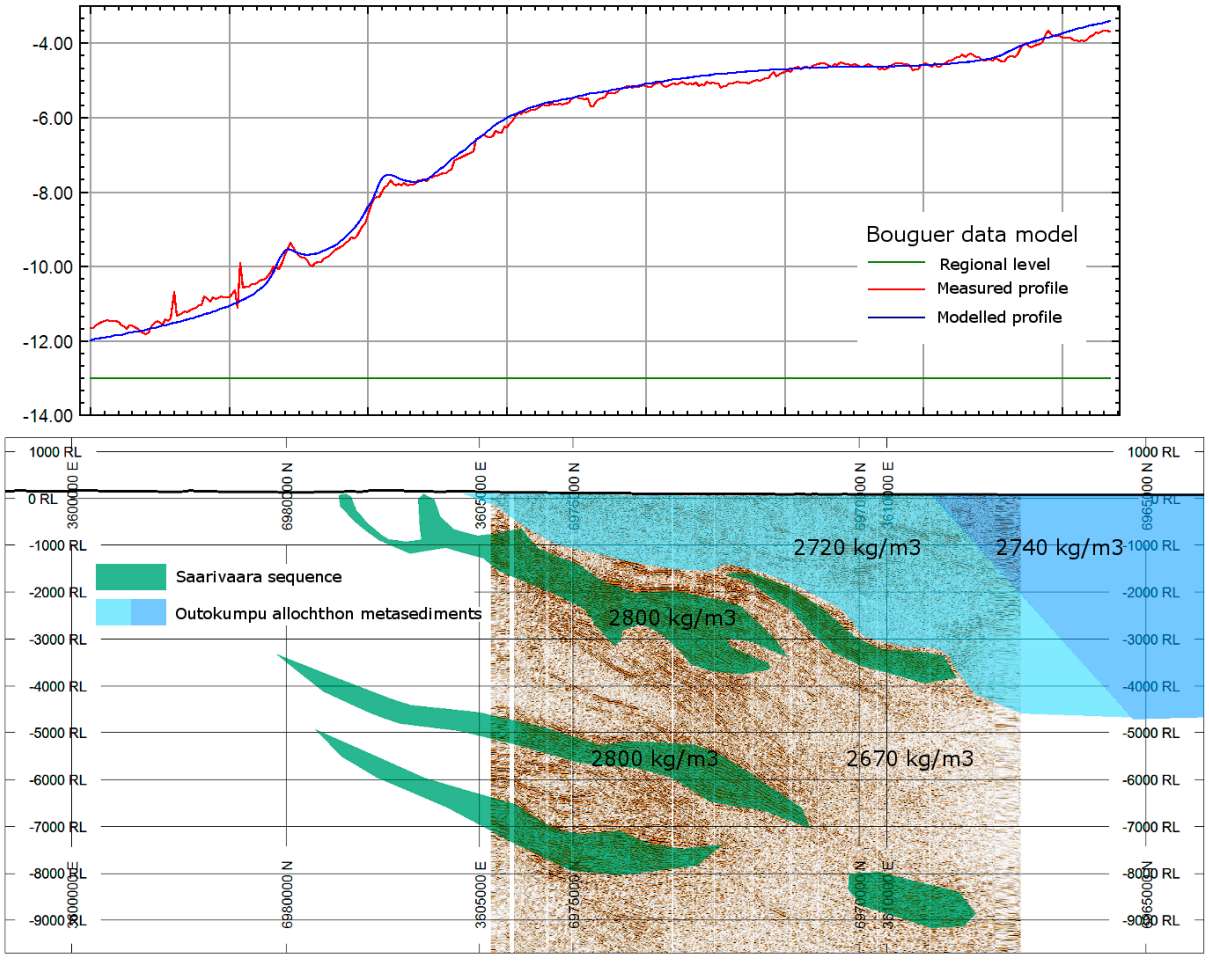


Fig. 14. Bouguer anomaly model along seismic profile V7 (after Heinonen et al. 2016 (this volume)).

was used as the background density value for the model.

For seismic profile V8, the measured gravity profile shows a large, long-wavelength maximum between the profile ends (Fig. 13). The first model bodies to enter in the model were the deep-plunging high reflectivity bodies, named here as Saarivaara reflectors and constructed after the seismic profile images; they produce a major part of the total Bouguer anomaly at the NW end of the profile. The metasediments are on average heavier than the granitoids (Fig. 7, Table 2), and thus contribute to the long-wavelength maximum between the granitoid minima; as the strong reflectors more or less disappear towards the southeast, their absence is compensated in the model by the thickening metasediment layer. The SE-dipping Outokumpu Belt formation shows as a local gravity maximum 23–25 km from the NW end of the profile.

The density of the metasediment formation in the model varies between 2720 and 2740 kg/m$^3$ so that the SW part of the formation is heavier. The density values for metasediments in the model are thus slightly lower than metasediment values in the drill holes (Table 3), suggesting that the rocks labelled as metasediments in the Outokumpu Belt may be slightly heavier than the metasediments regionally.

The V7 profile model (Fig. 14) is described in detail by Heinonen et al. (2016, this volume). The data on this profile were collected with denser sample spacing than the data used for modelling V8, but with the deep structure responses, the effect of sample spacing on the model is quite insignificant.

## Deposit-scale modelling examples

### Keretti profile: magnetic and gravity interpretation

No systematic gravity data exist or remain in the Outokumpu Oy gravimetric database for the historic Keretti mine (see Fig. 6). However, as it is probably the best place to validate the density parameters for chrysotile serpentinites due to both the abundance of serpentinites and the well-known geological constraints, one of the new gravity profiles (Fig. 6) was measured across the Outokumpu Belt at Keretti.

The new gravity data were jointly modelled with vertical component magnetic data (profile 185.400) from the data archives of Outokumpu Oy. The locations of the new gravimetric profile and the magnetic profile are indicated in Figure 15. The map also plots soil thickness readings derived from the drill-core database; they show values as high as >50 m in the mid-part of the gravity profile. This NE-trending region (Sumppi) is part of the Outokumpu/Keretti mines tailings area (e.g. Tornivaara & Kauppila 2014). Even though the region has been reworked since drilling, it can be assumed that in the mid-part of the profile, the soil cover can reach thicknesses of dozens of metres, and this information should be included in the model.

The physical/geological model (Fig. 16) comprises three rock classes (excluding the model background rock mica schist) and the soil cover, assumed to be wet sand with a density of 2000 kg/m$^3$ (Parasnis 1971). The density values for the model rocks were selected according to median values in Table 3 and magnetic susceptibilities estimated from Figure 9. As remanent magnetization parameters are known only for the black schists (BS) (Table 4), the values were included in the model. However, in the course of modelling, the Koenigsberger ratio (Q) values were increased from eight to fifteen, as this improved the model fit; the Horsmanaho data example (Fig. 10) shows that for black schists, values of Q > 10 are also well justifiable.

Two nearby cross-profiles of Koistinen (1981) were used as geological constraints (Fig. 17). All model bodies were extended 1500 m away from the profile in both directions.

The magnetic model response in Figure 16 highlights the importance of understanding the role of remanent magnetization as an anomaly source. Assuming the remanent magnetization parameters were not known, i.e. the magnetization of black schists was assumed to be caused by induced magnetization only (model profile $Q_{bs}$ = 0), it is practically impossible (considering the geological constraints and the measured susceptibility range) to match the model response to the observed values. However, as soon as the remanent magnetization parameters are included (model profile $Q_{bs}$ = 15), the model response amplitudes increase significantly and the modelled response conforms significantly better to the observed data.

On the gravimetric profile, the 2.5-mgal minimum is largely caused by the low-density chrysotile serpentinite (SP) body, but the rather thick soil cover in the Sumppi region also contributes to the minimum. On this profile, OUM and BS rock class

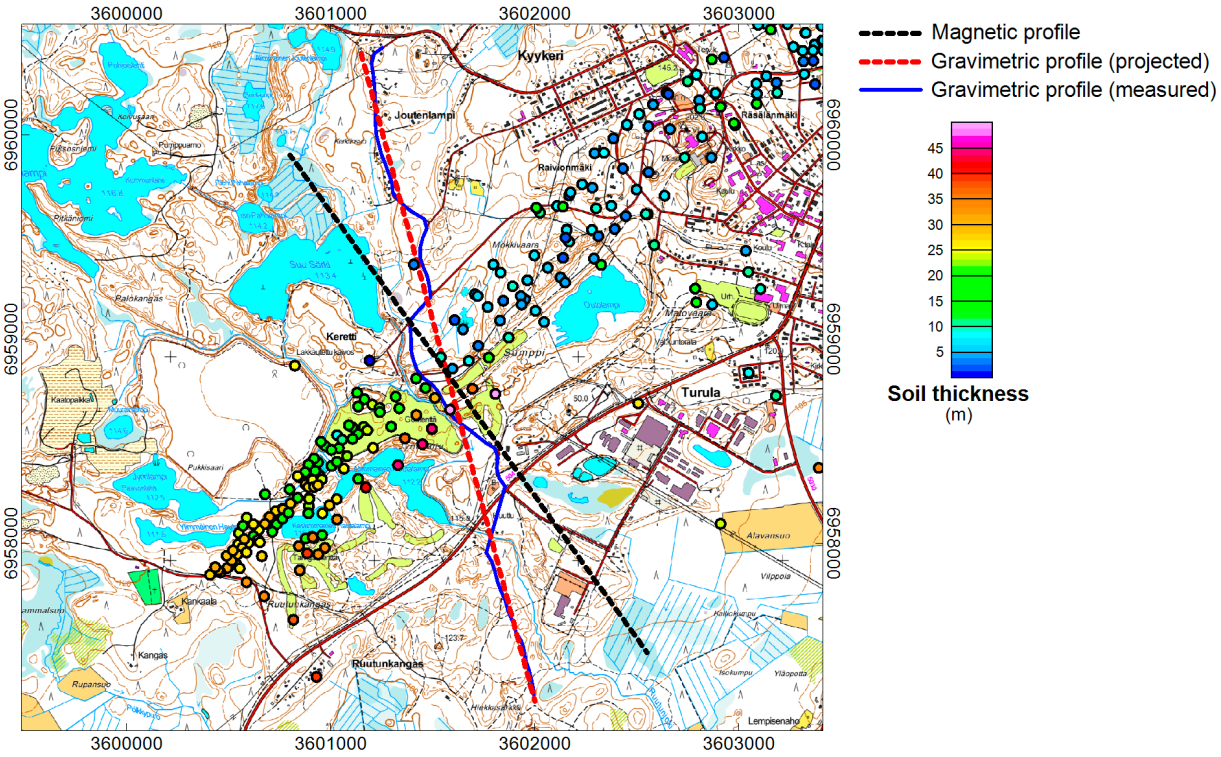


Fig. 15. Keretti modelling profile locations and soil thicknesses (as circle symbols) based on the drill-core database. Contains data from the National Land Survey of Finland Topographic Database 03/2013.

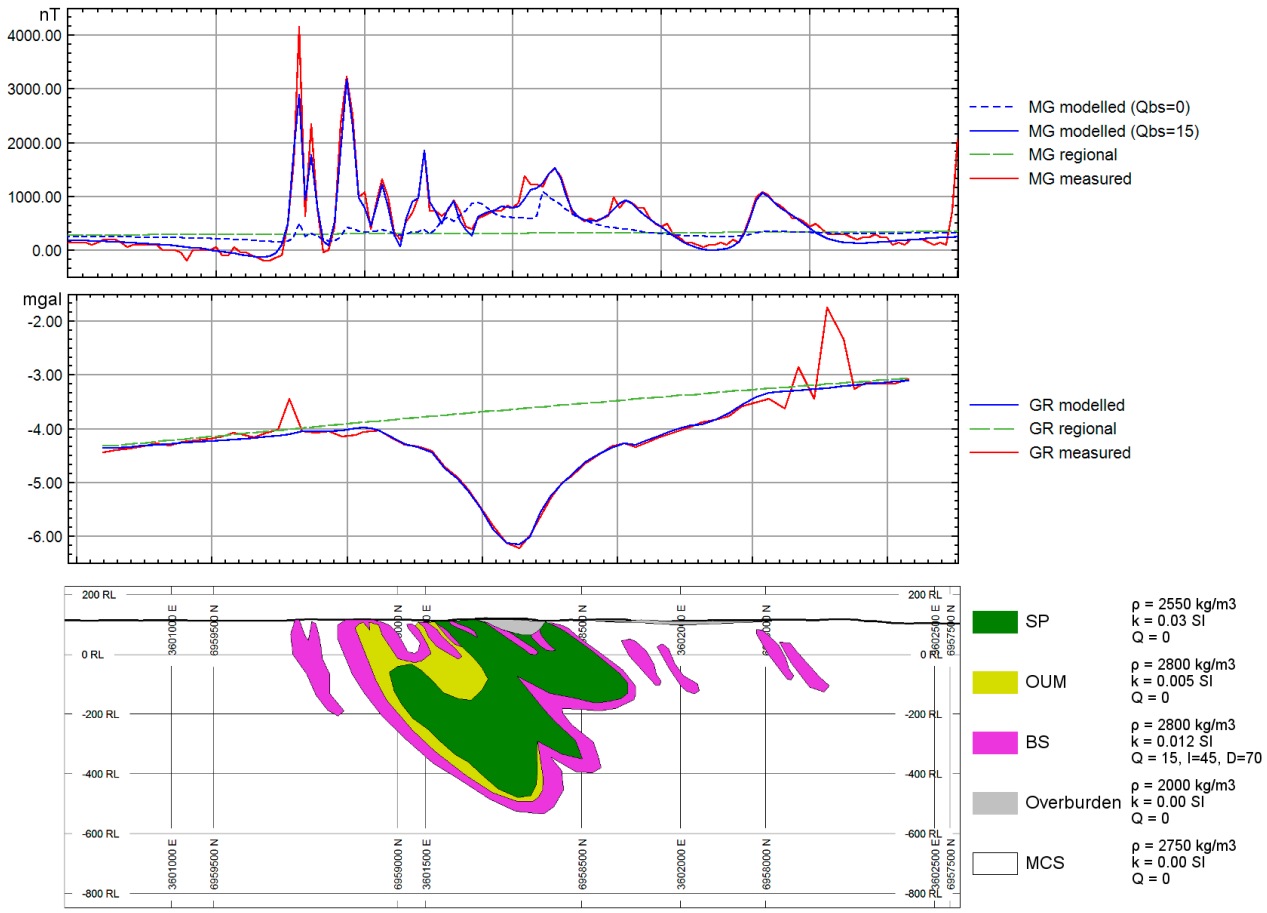


Fig. 16. Joint magnetic (MG, model profiles on the top) and gravity (GR, model profiles in the middle) forward model over Keretti (model bodies on the bottom). Rock class abbreviations as per Table 1; ρ = density, k = magnetic susceptibility, Q = Koenigsberger ratio.

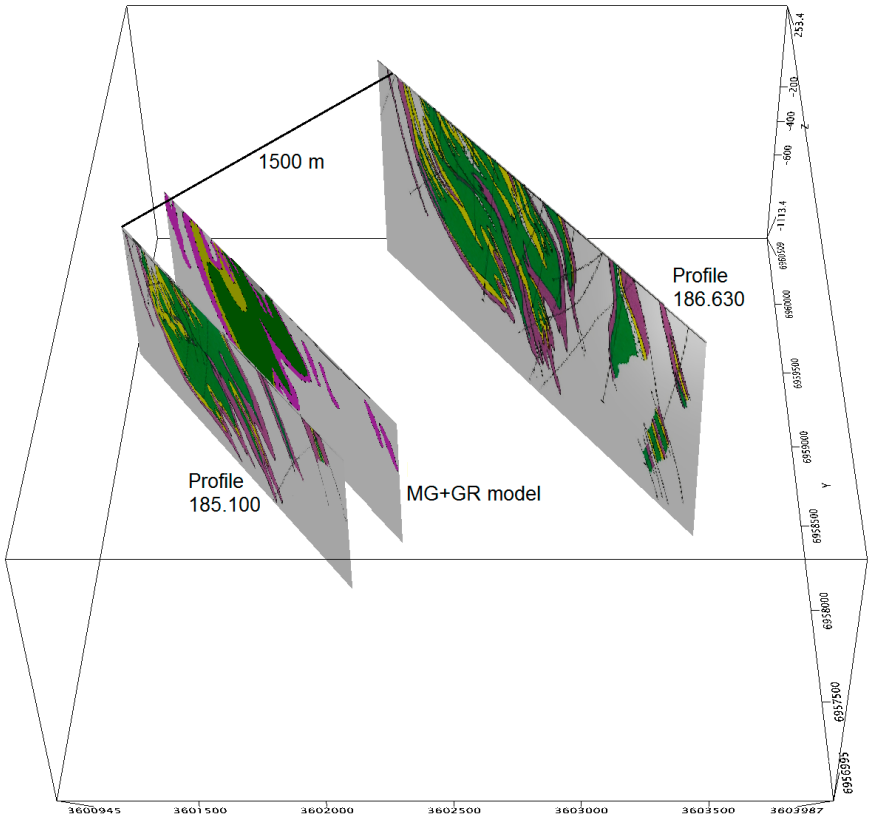


Fig. 17. Model cross section (MG+GR) in comparison to the geological profiles 185.100 and 186.630 of Koistinen (1981).

model densities are identical, and thus here the two rock classes cannot be distinguished from each other by gravity modelling.

### Kylylahti model

The isolated gravity anomaly in the Outokumpu Oy systematic ground survey data over Kylylahti (see location in Fig. 6) was interpreted with 3D inversion. Contrary to the conventional 2D and 3D forward modelling of previous examples, which calculates the theoretical response of a given subsurface property distribution, inversion results in a model that predicts the property distribution for a given observed response. The UBC-GIF GRAV3D inversion algorithm (Li & Oldenburg 1996), when run without any constraints, can be used for a quick, first-pass estimation of the gravity distribution, but for a more careful and realistic end result it is advisable to apply physical and/or geological constraints to inversion (e.g. Williams 2006).

The observed gravity data (Pekkarinen & Rekola 1994) contain vertical component gravity data collected with 50–100-m line spacing and 20-m sample spacing (Fig. 18A). The data lines were reorganised and the data microlevelled to improve the quality. The total value range in the dataset is ca. 4.5 mgal (Fig. 18B). Much of the response at the lower end of the range results from the regional long-wavelength feature in the southeast, caused by the low-density Sotkuma granite gneiss formation (Fig. 1). Prior to inversion, the regional trend must be subtracted from the observed data. The resulting residual anomaly (Fig. 18C) has its maximum at ca. 2.5 mgal.

In this study, the inversion constraints were based on the drill-core densities in the vicinity of the ore zone (Fig. 19) provided by Boliden Kylylahti. The drill-core data extend from the northern shallow drill holes along the ore zone to the depth of ca. 850 m, penetrating the deepest of the three separate mineralizations, the Wombat ore (Altona Mining Limited 2014). Two high-density zones can be identified in the density dataset, one related to the main mineralization zone by the eastern contact of the Kylylahti formation and the second to a shallower black schist zone; the densities of black schists in the Kylylahti region are notably higher than elsewhere in Outokumpu (Pekkarinen & Rekola 1995; Table 3).

Based on the drill-core densities, three mutually excluding density zones were extracted from

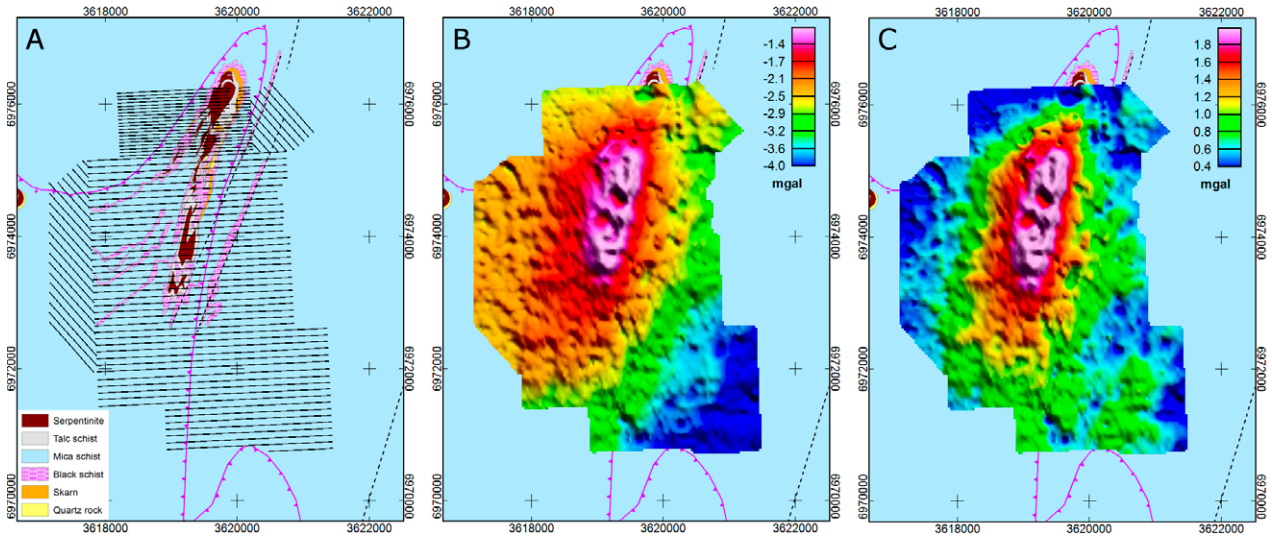


Fig. 18. A) Survey lines on a geological map (Bedrock of Finland – DigiKP), B) observed gravimetric data, C) residual data after regional trend removal.

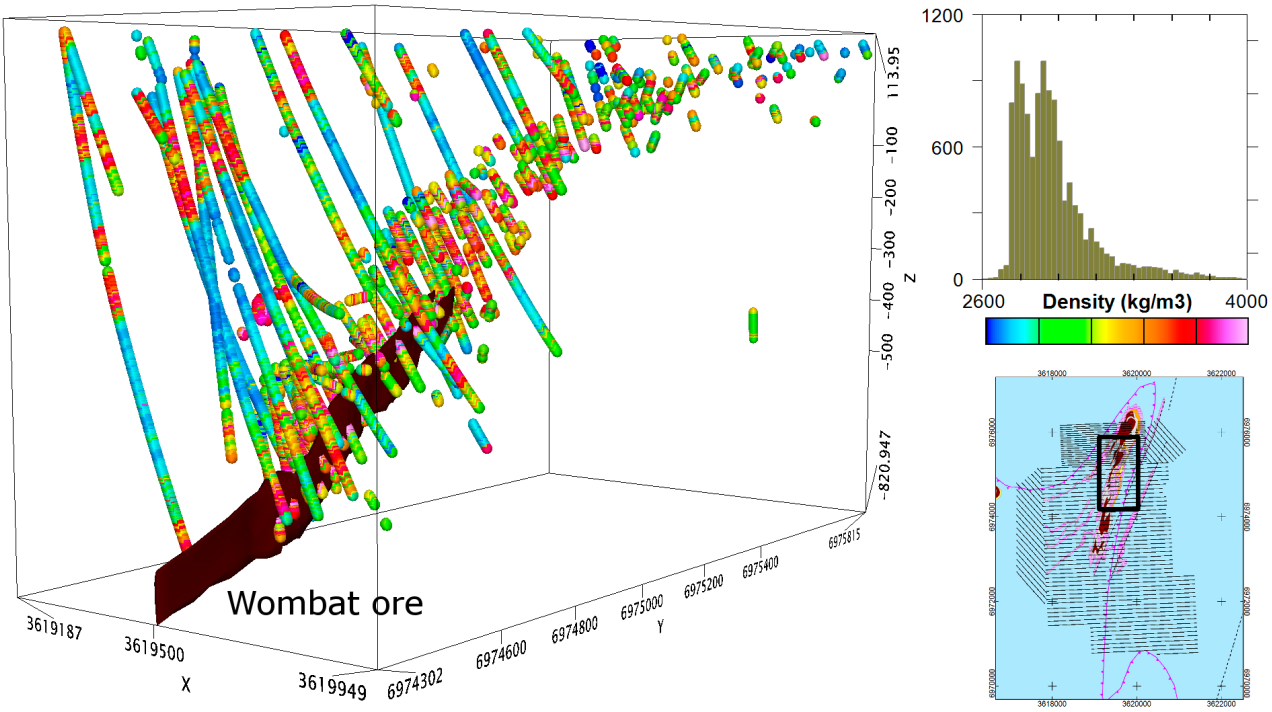


Fig. 19. Drill-core densities in the vicinity of the mineralised zone (viewed from southeast). Drill-core data and ore body model courtesy of Boliden Kylylahti. The geological map with gravity survey lines (bottom right) outlines the surface projection of the drill holes (black rectangle).

the data and used as inversion constraints (Fig. 20; values presented relative to to the density ($\rho$) of 2750 kg/m$^3$ (2.75 g/cm$^3$), the common density value of mica schist in Outokumpu (Table 3)). The constraints were included in the inversion as subregions where the recovered density is not allowed to vary outside the density boundaries indicated by the constraint. Outside the constraining density zones, i.e. in the unconstrained part of the inversion volume, the density is allowed to vary in the range $-1.0 \leq \rho \leq 1.0$ g/cm$^3$. Inversion parameters are presented in Table 6.

To validate the effect of the applied constraints, the inversion was also run without constraints (with the universal allowed value range of $-1.0 \leq \rho \leq 1.0$ g/cm$^3$). Comparison between the con-

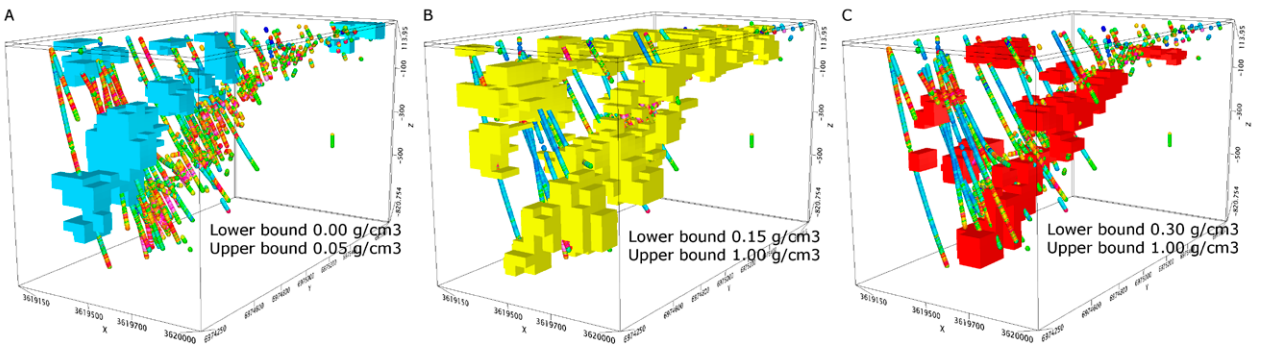


Fig. 20. Density zones corresponding to inversion constraints. A) True densities 2.75–2.78 g/cm³, B) true densities over 2.95 g/cm³, C) true densities over 3.1 g/cm³.

Table 6. GRAV3D parameters for the Kylylahti gravity inversion.

| Inversion parameter | Value |
|---|---|
| Mesh size | 100 x 120 x 100 cells (excluding padding) |
| Cell size | 50 x 50 m, cell height increasing downwards |
| Maximum depth | 5000 m |
| Data error | 0.1 mgal |
| Chifact | 0.5 |
| Topography level | 100 m |
| Depth weighting | $\beta = 2.0$, $z_0 = 51.00$ |
| Initial and reference models | 0.0 mgal |

strained and unconstrained results (Fig. 21) demonstrates that the selected constraints have a crucial effect on the results. The constrained model shows the two high-density zones in the densely drilled region (marked as a constraint region in Figure 21A) as expected, but in addition, it also shows better continuity of features in the regions where constraints do not apply. The unconstrained model is not able to separate between the two high-density zones, but goes for the simplest solution, that is, a single high-density structure that shows little correlation with the drilling results. Based on this, the southern high-density structure outside the constraint region in Figure 21A may just as well be divided in several parts, but the inversion is unable to separate between the parts. The necessary constraints could possibly be constructed based on the crossing reflection seismic profile V1.

Three north–south cross-sections of the constrained model (Fig. 22) highlight the main features in more detail. In the ore zone (A) and the shallow black schist zone (B), the model shows densities ≥ 3.0 g/cm³ due to the initial constraints; in the western section (C), the two high-density features are effectively solved unconstrained, as no or very few drill holes with density data are available in this section. The features most likely represent an imprecise, smoothed version of the actual physical value distribution.

### Synthetic example

The constrained Kylylahti inversion model provides an opportunity to examine the theoretical change in the gravimetric Bouguer anomaly response as a function of source depth in the case of the high-density Outokumpu association rocks. Figure 23 shows the forward modelled gravity response of the 2-km-deep 3D density mesh extracted from the top part of the Kylylahti constrained inversion model and transferred to various depths. With the top of the structure at the surface (depth 0 m), the corresponding anomaly amplitude is ca. 2 mgal. As the source is moved deeper, the amplitude naturally attenuates; were the top of the formation located at 500 m depth, the corresponding anomaly could still be separated from the background level, but at 1000 m depth the low amplitude and longer wavelength already make the task more challenging. Below 1000 m, it would be difficult to distinguish the response of the formation from the regional level, especially with there is any noise included in measurement data.

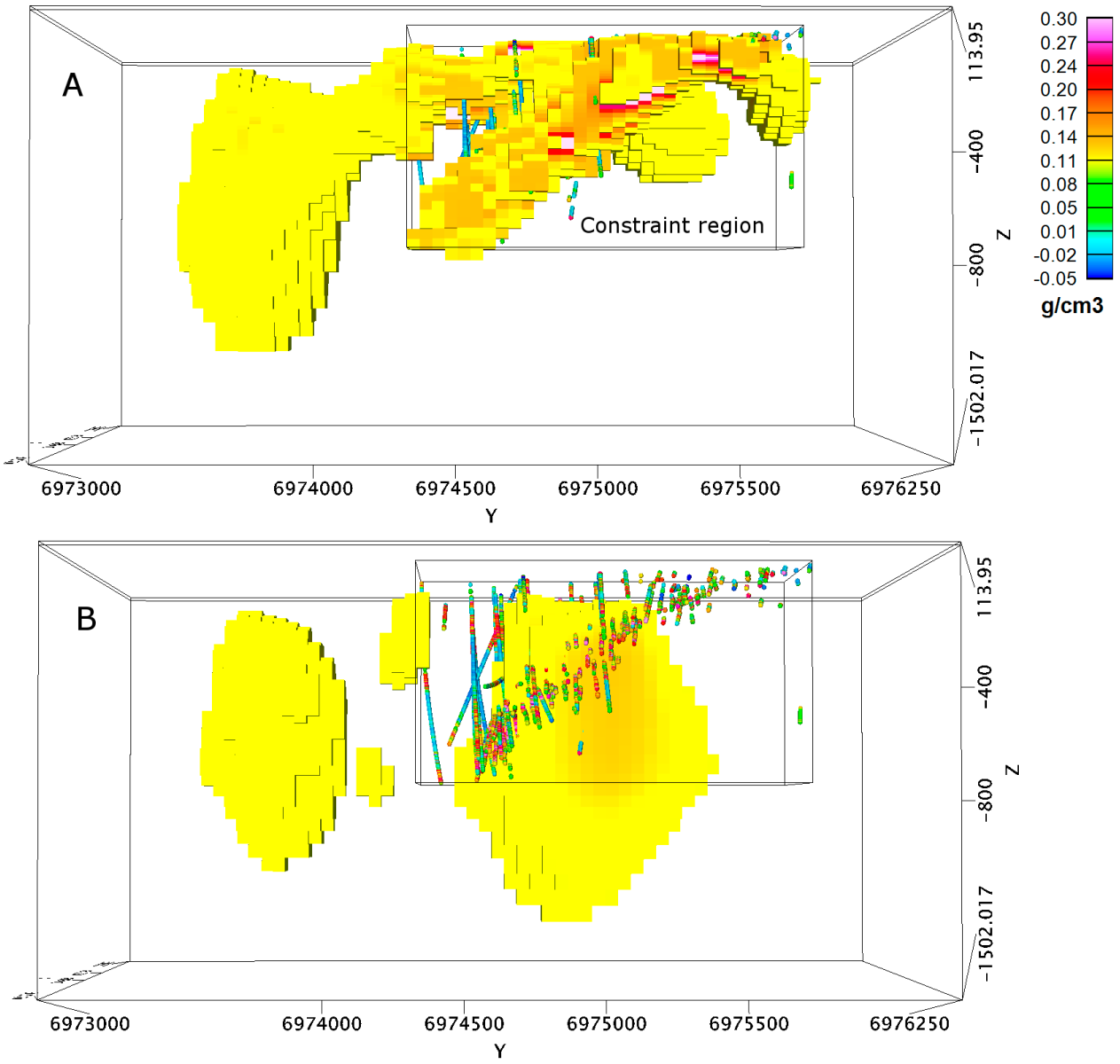


Fig. 21. The general shape of high-density structures according to the constrained (A) and unconstrained (B) recovered inversion models clipped at 0.1 g/cm³ in the vicinity of the Kylylahti mine (viewed from the east).

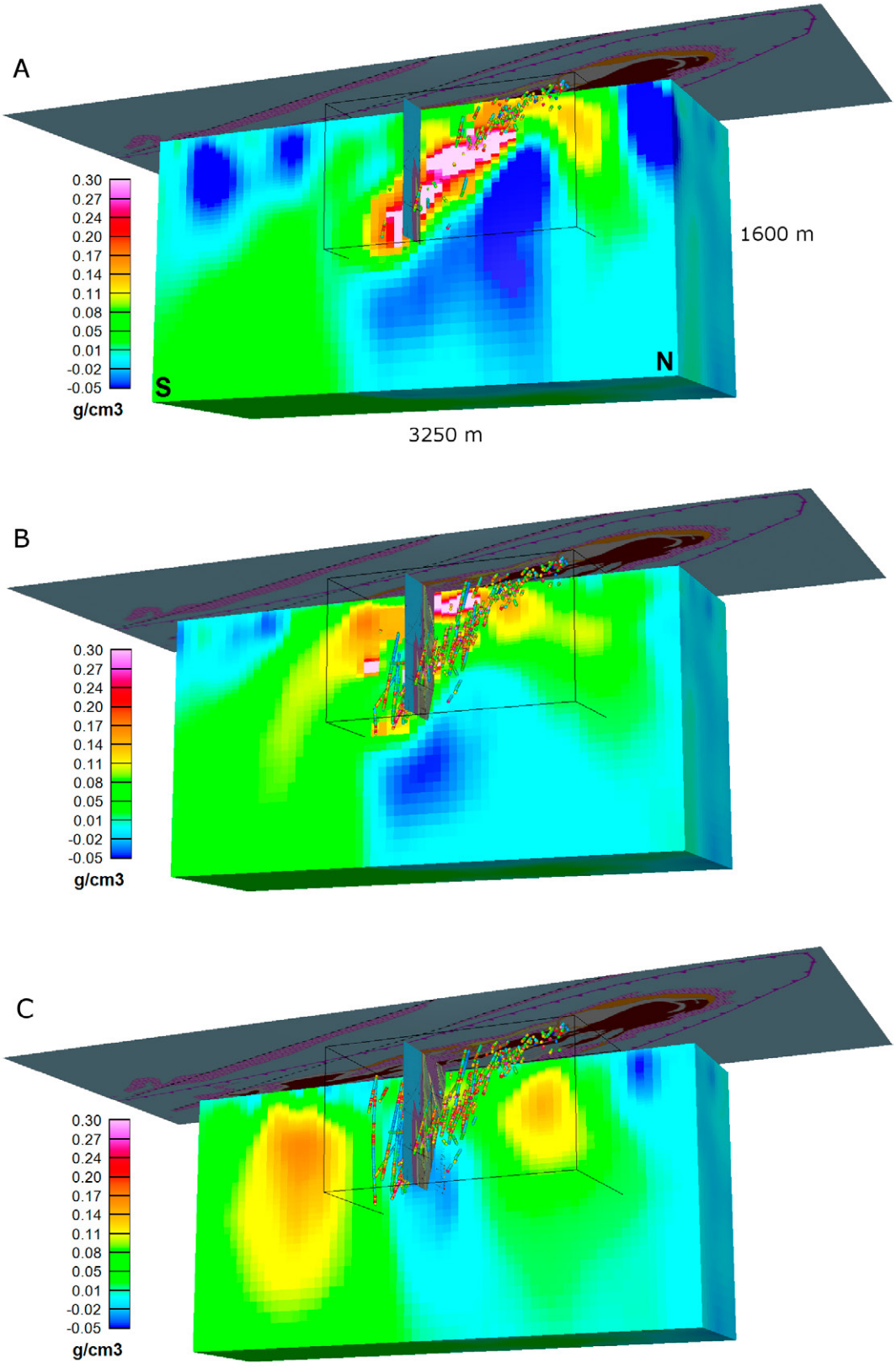


Fig. 22. Constrained inversion model clipped with NS plane A) E=3619650, B) E=3619450, C) E=3619200, together with a surface geological map (Bedrock of Finland – DigiKP), geological cross-section (Kontinen et al. 2006) and drill-core densities courtesy of Boliden Kylylahti.

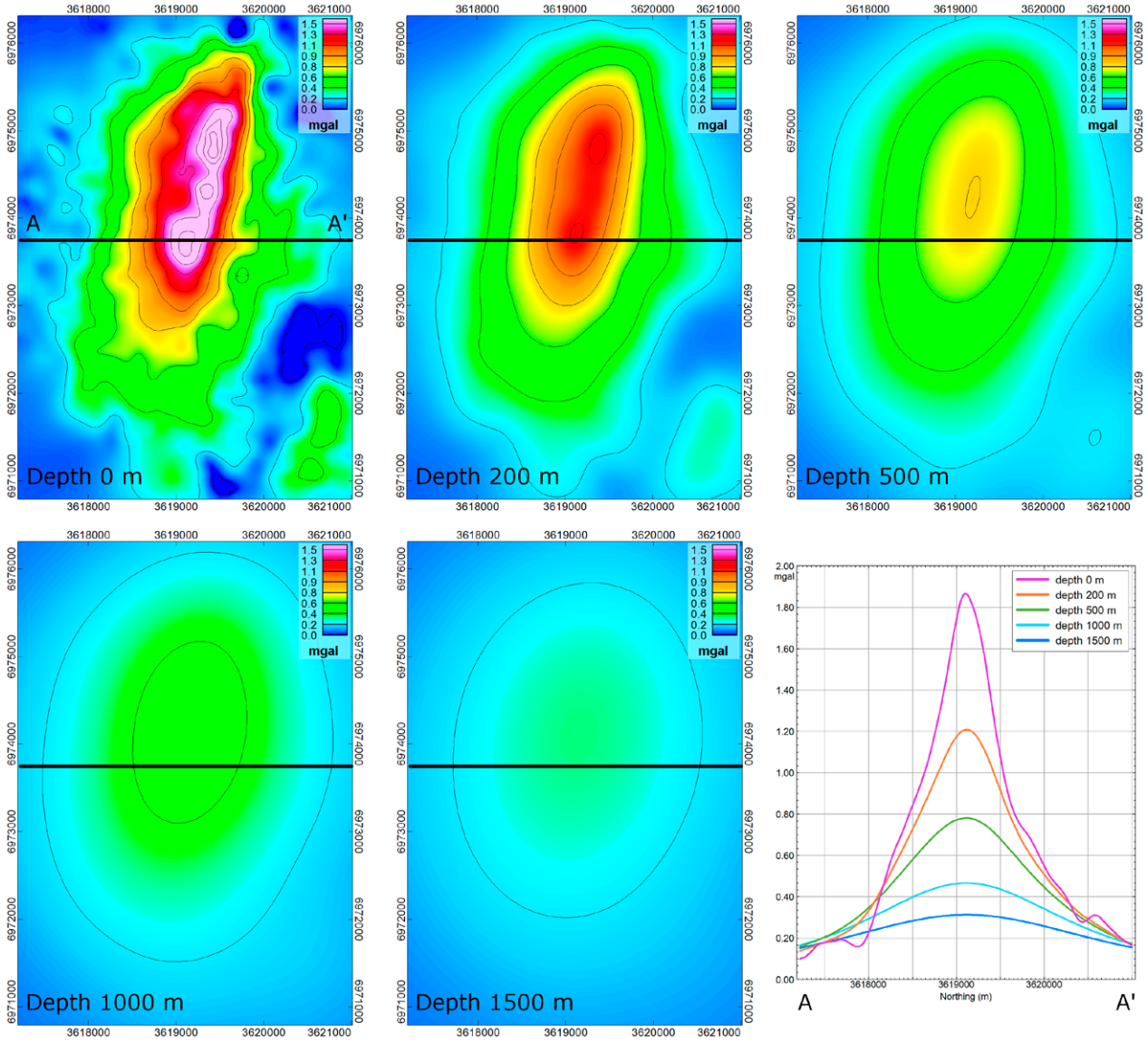


Fig. 23. The modelled gravity response of the Kylylahti formation located at various depths (depth values indicate the top of the formation). Data contours at 0.2-mgal intervals.

## DISCUSSION

A major part of this study focused on the classification and grouping of the large petrophysical drill-core sample datasets available for the Outokumpu-Miihkali region. When connected to modelling, petrophysical data cannot be treated as a solitary dataset, but need to be evaluated together with other sample qualifiers. In order to manage, classify and analyse the data for modelling purposes, the rock type and location of samples need to be correctly defined. It is therefore not only the quality of the petrophysical measurements performed on samples, but also the quality and accuracy of other qualifiers that is essential for a successful modelling outcome.

The historical data used in this study have been generated over several decades of exploration in the Outokumpu region. Inevitably, lithological definitions for the drill-core samples, in particular, show great diversity. The work performed in the GEOMEX project in standardizing and documenting the rock classes in the drill-core database is noteworthy. Without their antecedent efforts it would not have been possible to complete the petrophysical classification presented in this study.

The choice of data classification scheme in this study was based on major rock classes and rock combinations typical of the Outokumpu association. It may be justifiably argued that, for example,

the OUM class containing carbonate rocks, skarns and quartz rocks should be subdivided in petrophysical analysis, as the densities of the rock types within the class diverge from each other. However, the subjective choice of combining the rock classes in the way presented in this study was based on the available geological cross-sections: the aim was to have the geophysical models equate to the existing geological models with reasonably sized modelling units.

The importance of including all available geological and geophysical background knowledge in the modelling/inversion process is evident, especially when dealing with low-amplitude responses from deep-set sources. In the Outokumpu region, density modelling is better controlled than magnetic modelling: the significant amount of remanent magnetization, especially in black schists but also in other rocks, can easily lead the modeller astray, as even today the remanent magnetization parameters are only known on a general level. Modelling examples demonstrated that with the help of background data and constraints, gravity modelling can detect sources at depths of several kilometres; however, the geological nature of these sources is not easily resolved. When the sources are set deeper or the density distributions become more complex, the roles of reliable constraints and integration of data in an effective 3D modelling environment increase.

## CONCLUSIONS

The data from petrophysical drill-core samples from the Outokumpu brownfield mining camp, collected over several decades of exploration, were re-classified and reanalysed in this study. In addition to lithological classification, the data were also grouped by location, because, mainly due to the changing metamorphic grade, the Outokumpu Belt and its vicinity cannot be treated as a homogeneous region with regard to any of the rock unit's physical parameter ranges.

In the Outokumpu Belt and Miihkali, serpentinites are present in the Outokumpu assemblage throughout the region. Due to metamorphic zoning and the resulting mineral compositions, their densities vary from ca. 2560 kg/m$^3$ in the southwest to ca. 2760 kg/m$^3$ in the northeast. At the high end of the density range, the sulphide ore in Kylylahti has a median density of 3450 kg/m$^3$. The talc-carbonate rocks and talc schists and the rest of the rocks of ultramafic origin have densities of ca. 2800–2850 kg/m$^3$, and locally even 2900 kg/m$^3$. The metabasites, most prominent in Miihkali, have there densities of 2920 kg/m$^3$. The density range for the Outokumpu allochthon metasediments is narrowly constricted to values around 2750 kg/m$^3$ and for black schists around 2800 kg/m$^3$. Various granitoids (2600–2670 kg/m$^3$) are lighter than the allochthon metasediments that, in the regional gravity models presented in this study, give rise to a regional long-wavelength Bouguer anomaly between the granitoids in the Maarianvaara-Saarivaara region and Sotkuma.

Both forward modelling and inversion algorithms were applied in gravity modelling cases. The regional and deposit-scale modelling problems set in the study could all be reliably solved by applying the density parameters obtained from the petrophysical data together with available geological and geophysical constraints. Forward models for the seismic profiles V7 and V8 presented in the study have their deepest model bodies at depths of 8–9 km. However, as the response from these depths is already strongly attenuated, the model is at these depths a rather subjective interpretation of the seismic reflection image: detailing these sources without the constraints provided by the seismic data would be a challenge. Also, as shown by the V7 and V8 profile model cases with the Saarivaara reflector rocks that have the overall density similar to Outokumpu association rocks, reliably judging the yet unknown geological nature of other strong, deep reflectors on the profiles based on the long-wavelength response in the gravity data is a task that remains unresolved by petrophysical classification and potential field modelling.

In addition to density contrasts, the depth of detection also depends on the source body dimensions: a synthetic gravity modelling example indicates that a body with dimensions and properties similar to the Kylylahti formation, small in size in comparison to the massive reflectors on the seismic profiles, can be detected in gravity data from a depth of one kilometre or less.

All the rock classes show low to moderately high magnetic susceptibilities. Most of the induced magnetization originates from serpentinites and black schists. However, remanent magnetization often dominates over induced magnetization as the

magnetic anomaly source, as shown by the Keretti modelling example in this work. Including remanent magnetization as a petrophysical parameter is an aspect that warrants careful consideration in magnetic modelling on the region.

## ACKNOWLEDGEMENTS

The author would like to warmly thank A. Kontinen for his generous help and comments, which helped improve the manuscript. T. Ruotoistenmäki is thanked for sharing his experience of the geophysical characteristics of the Outokumpu region. S. Mertanen and T. Ahokas are acknowledged for reviewing the manuscript. Boliden Kylylahti and Mondo Minerals B.V. are thanked for providing petrophysical data for the study.

## REFERENCES

**Ahokas, T. 1980.** Petrofysikaalisia sovellusesimerkkejä. In: Pesonen. L. J. (ed.) Sovelletun geofysiikan jatkokurssi 1979–1980: ”Petrofysiikan sovellutuksia”. Otaniemi: Helsinki University of Technology. (in Finnish)

**Ahokas, T. 1984.** Vuonos – Kylylahti (ns. Papan putki) geofysikaalisista tutkimuksista. Outokumpu Oy. 11 p. (in Finnish)

**Airo, M.-L. & Säävuori, H. 2013.** Petrophysical characteristics of Finnish bedrock: Concise handbook on the physical parameters of bedrock. Geological Survey of Finland, Report of Investigation 205. 33 p.

**Airo, M.-L., Säävuori, H. & Vuoriainen, S. 2011.** Petrophysical properties of the Outokumpu Deep Drill Core and the surrounding bedrock. In: Kukkonen, I. T. (ed.) Outokumpu Deep Drilling Project 2003–2010. Geological Survey of Finland, Special Paper 51, 64–82.

**Altona Mining Limited 2014.** Kylylahti Resources Increased. ASX/Media Announcement, 26 March 2014.

**Bedrock of Finland – DigiKP.** Digital map database [Electronic resource]. Espoo: Geological Survey of Finland [referred 09.03.2016]. Version 2.0.

**Clark, D. A. 1997**. Magnetic petrophysics and magnetic petrology: aids to geological interpretation of magnetic surveys. AGSO Journal of Australian Geology & Geophysics, 17(2), 83–103.

**Elo, S. 2007.** Gravity Operations of the Geological Survey of Finland. In: Poutanen, M. & Koivula, H. (eds.) Geodetic Operations in Finland 2004–2007. Finnish Geodetic Institute, 33–36.

**Gaál, G. & Parkkinen, J. 1993.** Early Proterozoic ophiolite-hosted copper-zinc-cobalt deposits of the Outokumpu type. In: Kirkham, R. V., Sinclair, W. D., Thorpe, R. I. & Duke, J. M. (eds) Mineral Deposit Modelling. Geological Association of Canada, Special Paper 40, 335–341.

**Gaál, G., Koistinen, T. & Mattila, E. 1975.** Tectonics and stratigraphy of the vicinity of Outokumpu, North Karelia, Finland: including a structural analysis of the Outokumpu ore deposit. Geological Survey of Finland, Bulletin 271. 67 p.

**Hautaniemi, H., Kurimo, M., Multala, J., Leväniemi, H. & Vironmäki, J. 2005.** The “Three In One” aerogeophysical concept of GTK in 2004. In: Airo, M.-L. (ed.) Aerogeophysics in Finland 1972–2004: Methods, System Characteristics and Applications. Geological Survey of Finland, Special Paper 39, 21–74.

**Heinonen, S., Kontinen, A., Leväniemi, H., Lahti, I., Junno, N., Kurimo, M. & Koivisto, E. 2016.** Sukkulansalo National Test Line in Outokumpu: A ground reference for deep exploration methods. In: Aatos, S. (ed.) Developing Mining Camp Exploration Concepts and Technologies – Brownfield Exploration Project 2013–2016. Geological Survey of Finland, Special Paper 59. (this volume)

**Huhma, A. 1971.** Outokumpu. Geological Map of Finland 1:100 000, Pre-Quarternary Rocks, Sheet 4222. Geological Survey of Finland.

**Huhma, H. 1986.** Sm-Nd, U-Pb and Pb-Pb isotopic evidence for the origin of the Early Proterozoic Svecokarelian crust in Finland. Geological Survey of Finland, Bulletin 337. 48 p.

**Kääriäinen, J. & Mäkinen, J. 1997.** The 1979–1996 Gravity Survey and Results of the Gravity Survey of Finland 1945–1996. Publications of the Finnish Geodetic Institute 125. 24 p.

**Ketola, M. 1973.** Outokummun alueen geofysiikasta. Outokumpu Oy. 15 p. (in Finnish)

**Ketola, M. 1974.** Karttalehdellä 4313 suoritetun alueellisen gravimetraustuloksen tulkinta profiililla X=990.00. Outokumpu Oy. 2 p. (in Finnish)

**Ketola, M. 1979.** On the application of geophysics in the indirect exploration for copper sulphide ores in Finland. In: Hood, P. J. (ed.) Geophysics and Geochemistry in the Search for Metallic Ores. Geological Survey of Canada, Economic Geology Report 31, 665–684.

**Koistinen, T. J. 1981.** Structural evolution of an early Proterozoic stratabound Cu-Co-Zn deposit, Outokumpu, Finland. Transactions of the Royal Society of Edingburgh: Earth Sciences 72(2), 115–158.

**Kontinen, A. & Säävuori, H. 2013.** Geological correlation and significance of the prominent Saarivaara reflector from the HIRE V7 vibroseismic survey in the Outokumpu area. In: Hölttä, P. (ed.) Current Research: GTK Mineral Potential Workshop, Kuopio, May 2012. Geological Survey of Finland, Report of Investigation 198, 81–85.

**Kontinen, A., Peltonen, P. & Huhma, H. 2006.** Description and genetic modelling of the Outokumpu-type rock assemblage and associated sulphide deposits. Final technical report for GEOMEX J.V., Workpackage Geology. Geological Survey of Finland, archive report M10.4/2006/1. 378 p.

**Kukkonen, I. T. (ed.) 2011.** Outokumpu Deep Drilling Project 2003–2010. Geological Survey of Finland, Special Paper 51. 252 p.

**Kukkonen, I. T. & Lahtinen, R. (eds) 2006.** Finnish Reflection Experiment FIRE 2001–2005. Geological Survey of Finland, Special Paper 43. 247 p.

**Kukkonen, I. T., Heikkinen, P., Heinonen, S. Laitinen, J. & HIRE Working Group of the Geological Survey of Finland 2011.** Reflection seismics in exploration for mineral deposits: Initial results from the HIRE project. In: Nenonen, K. & Nurmi, P. A. (eds) Geoscience for Society: 125th Anniversary Volume. Geological Survey of Finland, Special Paper 49, 49–58.

**Kukkonen, I. T., Heinonen, S., Heikkinen, P. J. & Sorjonen-Ward, P. 2012.** Delineating ophiolite-derived host rocks of massive sulfide Cu-Co-Zn deposits with 2D high-resolution seismic reflection data in Outokumpu, Finland. Geophysics 77, WC213-WC222.

**Lahti, I., Leväniemi, H., Kontinen, A., Sorjonen-Ward, P., Aatos, S. & Koistinen, E. 2016.** Geophysical surveys of the Miihkali area, Eastern Finland. In: Aatos, S. (ed.) Developing Mining Camp Exploration Concepts and Technologies – Brownfield Exploration Project 2013–2016. Geological Survey of Finland, Special Paper 59. (this volume)

**Lehtonen, T. 1981.** Outokummun alueen kivilajien petrofysikaalisista ominaisuuksista. Unpublished master's thesis, Helsinki University of Technology. 77 p. (in Finnish)

**Li, Y. & Oldenburg, D. W. 1998.** 3-D inversion of gravity data. Geophysics 63, 109-119.

**Mäkelä, M. 1983.** Outokumpu-jakso ennen ja nyt. Vuoriteollisuus – Bergshanteringen 1/1983, 18-22. (in Finnish)

**Outokumpu News 3/82.** How to explore deep-seated ores. Outokumpu Oy, 4-7.

**Parasnis, D. S. 1971.** Principles of Applied Geophysics, Third edition. Chapmann and Hall Ltd. 275 p.

**Pekkarinen, L. & Rekola, T. 1994.** Raportti Polvijärven Kylylahden alueen malmitutkimuksista 1992-1994. Outokumpu Finnmines Oy, Exploration report. 26 p. (in Finnish)

**Peltonen, P., Kontinen, A., Huhma, H. & Kuronen, U. 2008.** Outokumpu revisited: New mineral deposit model for the mantle peridotite-associated Cu-Co-Zn-Ni-Ag-Au sulphide deposits. Ore Geology Reviews 33, 559-617.

**Ruotoistenmäki, T. & Tervo, T. 2006.** Geophysical characteristics of Outokumpu area, SE Finland. Geological Survey of Finland, Report of Investigation 162. 37 p.

**Rekola, T. & Hattula, A. 1995.** Geophysical surveys for strata-bound Outokumpu-type CU-CO-ZN deposits at Kylylahti, Eastern Finland. Exploration Geophysics 26, 60-65.

**Säntti, J., Kontinen, A., Sorjonen-Ward, P., Johanson, B. & Pakkanen, L. 2006.** Metamorphism and Chromite in Serpentinized and Carbonate-Silicate-Altered Peridotites of the Paleoproterozoic Outokumpu-Jormua Ophiolite Belt, Eastern Finland. International Geology Reviews 48, 494-546.

**Tornivaara, A. & Kauppila, P. 2014.** Kaivoksen sulkeminen ja jälkihoito: Ekskursio Luikonlahden ja Keretin kaivosalueille. Geological Survey of Finland, Guide 60. 35 p. (in Finnish)

**Williams, N. C. 2006.** Applying UBC-GIF potential fiels inversions in greenfields or brownfields exploration. Australian Earth Sciences Convention, Melbourne, Australia, ASEG/GSA, Abstracts.